JWST TECHNICAL MEMORANDUM

Title: **OTE Science Performance Memo 1** *JWST Line-of-Sight Jitter Measurement during Commissioning*	Doc #: JWST-STScI-008271 Date: 27 September 2022 Rev: -
Authors: George Hartig and Matt Lallo	Release Date: 15 November 2022

Table of Contents

Operated by the Association of Universities for Research in Astronomy, Inc., for the National Aeronautics and Space Administration under Contract NAS5-03127

List of Figures

List of Tables

1.0 INTRODUCTION

An important aspect of the observatory performance is its Line-of-Sight (LOS) pointing stability over both longer, observation length intervals (drift) and over much shorter time scales (jitter). The top-level Observatory specification for LOS stability is ~7 mas RMS (per axis, SI-dependent) over 15 s, with contributions from many sources, including the closed-loop guiding performance of the FGS and ACS and excitations from the mechanical moving parts of the observatory, especially the reaction wheel assemblies (RWAs) and the MIRI Cryo-Cooler (CC) subsystem. Special tests were included in the commissioning plan to specifically assess the CC contribution to LOS jitter. Refer to Sec 4 for a description of these tests and their results. There is no dedicated test for the RWA contributions; these are assessed by frequency (PSD) analyses over the many instances of the jitter measurements, as the wheel speeds vary during the course of the commissioning program.

As OTE commissioning drew to a close and in the ensuing maintenance epoch, the LOS jitter continues to be monitored using the routine WFSC maintenance observations by including LOS measurements along with the weak lens Fine Phasing measurements, with OTE-26 (CAR 71.n, PID 1163) and its Cycle-1 calibration program counterparts. The Fine Phasing APT template incorporates this LOS measurement capability. Sec 5 describes these measurements and results, to date. Appendix B presents a table of these measurements, their execution date/time, input files, RWA and CC parameters and resulting jitter estimates.

The original analysis tool for the CC LOS jitter assessment is MATLAB code provided by NGAS and installed on the WSS workstation. It provides RMS jitter and PSD plots as well as plots of the CC system parameters and the RWA speeds, and logs some of the results in a csv file. An additional tool (***jita.pro***), developed in-house by the author and written in IDL, has also been provided for these analyses, and offers more extensive data quality assessment and frequency analysis capabilities. The ***jita*** tool has become the standard as commissioning progressed. These tools, their usage and output products, are described in Sec 3.

2.0 MEASUREMENT METHODS

The LOS jitter measurements are made using the NIRCam module A SW 8x8 px subarray, on SCA A3, which is read out with the RAPID pattern in 2.2 ms intervals to yield a time series of PSF images at high enough frequency (<230 Hz) to detect jitter induced by the expected modes of OTE vibration. Use of Module B, SCA B4 is also allowed, but is not in the baseline. The exposures are specified to use up-the-ramp sampling with at least 20 groups; fewer groups leads to more reset intervals, which affect the frequency analysis accuracy, as the gaps they cause in the time series must be interpolated over. Typical exposure times are 2-6 minutes, yielding 50k-150k samples. Longer exposures are precluded due to a frame count limitation of the ISIM FSW (<196,608).

For the Cryo-Cooler jitter assessment programs, in order to sample any changes that occur while the CC settles after each frequency change, multiple exposures were specified, with ~40s gaps, to cover ~20 minute observations; however, this was not exercised during commissioning when no frequency sweeps were required (see sec 4.1). The multiple exposure technique was used to good effect for the JT-assisted MIRI detector anneal jitter test (CAR-905); see Sec 4.2.

One of three bandpass filters may be selected in the APT Fine Phasing template (F212N, F210M and F200W), depending on the target brightness and the desired number of up-the-ramp frames (ngroups). Since these jitter measurements are "piggy-backed" with the Fine Phasing WF maintenance exposures, the target must be compatible with both to avoid unnecessary slewing between targets. For most of the OTE-26 (CAR 71.n) measurements, K~9 targets were used with the F210M filter and 60 groups, with full-diversity FP exposures. Later, to improve observing efficiency, WLPM8-only diversity was selected, permitting shorter exposures with K~7 targets and the concomitant change in LOS jitter exposures to use F212N and 72 groups.

The image data, processed only through stage 1b (uncal), are provided by DMS to the WSS workstation with a DAN. Similarly, there is a standing order for FOS processing of the associated engineering data to produce a FOF (.csv) file of the relevant CC and RWA operating parameters and delivery to the WSS workstation, with a DAN. Both the NGAS and ***jita*** analysis tools require this engineering FOF file to perform their analyses and data logging.

3.0 ANALYSIS METHODS

Analysis of the LOS jitter data is identical for both CC evaluation OTE-24 and OTE-33 data sets, as well as for routine monitoring (OTE-26) and the MIRI JT-assisted anneal studies (CAR MIRI-081, PID 1439). Both the NGAS-supplied CC jitter tool and the auxiliary IDL ***jita*** tool were initially used to process the data and their results compared. Typically, the WSS operator used the NGAS tool, while the Shadow operator used ***jita***. These analyses began after the DMS-processed science data were received, with an accompanying DAN, at the WSS workstation *and* the associated FOF file of relevant telemetry was received, also at the WSS workstation, with an accompanying DAN. If the latter was not received in timely manner, the FOF file could be manually created using ATOM and the appropriate telemetry history filter file, *ote_ccj_data.xml*, located in the cm directory.

To achieve the desired maximal temporal resolution, the up-the-ramp frames are differenced to produce ngroups-1 images, effectively bias-subtracted with 2.2 ms exposures, for each of the many integrations specified to cover the nominal ~ 2 minute measurement period. The PSF position is measured for each of these (typically >50000) samples using one of several techniques (2-D gaussian fit, cross-correlation, centroiding) and the statistics computed to return the RMS jitter in each axis, converting from pixels to mas using the NIRCam SW plate scale (31.1 mas/px) and RSS-ing these to compute the radial jitter.

For frequency analysis, to maintain a coherent time-series of measurements, the reset and initial frame intervals must be accounted for. The reset interval is slightly longer than the frame (group) time, at 2.36 ms, the extra time required for a "rolling-row" reset of the remainder of the SCA not being read out in the subarray. The ***jita*** tool then resamples on a 2.2 ms cadence using spline interpolation over the 4.56 ms gaps and then the fft is computed to determine the PSD. The NGAS tool does not account for the slightly longer reset interval.

The ***jita*** tool has been used for most of the commissioning analyses, since it provides greater functionality, but the NGAS tool remains available to use, if desired.

3.1 NGAS CCJ TOOL ANALYSIS

A step-by-step "How-to" tutorial on running the NGAS CCJ tool on the WSS workstation, with screen shots, is available at:

https://jwstitarwiki.stsci.edu/display/WFSCOWG/Cryocooler+Jitter+Analysis+Tool

Briefly, the tool is run on the WSS workstation with the following steps:

1. Invoke the tool by clicking the "Start CCJ Wizard" button
2. Select the science data and engineering data FOF files
3. Click "Start CCJ"
4. After the tool runs, returning "Success", click "Next"
5. Examine the list of output files for completeness: 11 png plots and a csv log file, as listed in Table 1.

Table 1. Output Products of the NGAS CCJ Tool

Filename	Description
CCJ_Output.csv	CCJ Output CSV File that lists the summary of the analysis
centroids_direct_<calSci>.png	Centroid Direct
energy_<calSci>.png	8x8 encircled energy
fits_data_mat.mat	Matlab output file
JT_Vibe_Harmnonics_<calEng>.png	JT Total Vibration Harmonics Magnitude
Motor_Drive_Mag_<calEng>png	Motor Drive Magnitude Time History
Motor_Frequency_<calEng>.png	Motor Frequency Set Point History
PT_Vibe_Harmnonics_<calEng>.png	PT Total Vibration Harmonics Magnitude Time History
RWA_Speeds_<calEng>.png	Reaction Wheel Speed Time History
Total_Vibe_Output_<calEng>.png	Total Vibration Output Time History (JT and PT)
Vibe_Loop_Counter_<calEng>.png	Vibration Algorithm Loop Counter
Vibe_Meas_Loop_Cntr_<calEng>.png	Vibration Measurement Loop Counter Time History
Vibe_Meas_Status_<calEng>.png	Vibration Measurement Status Time History (JT and PT)

The most useful plot is the "centroids_direct_<fn>", which displays the centroid (determined using a fft technique) in X and Y for each frame, the full range and RMS (1 sigma) jitter (in px) in the X and Y directions, as well as the PSD, with the JT and PT drive frequencies shown and the RWA frequencies over-plotted as multi-colored vertical bars (Fig. 1).

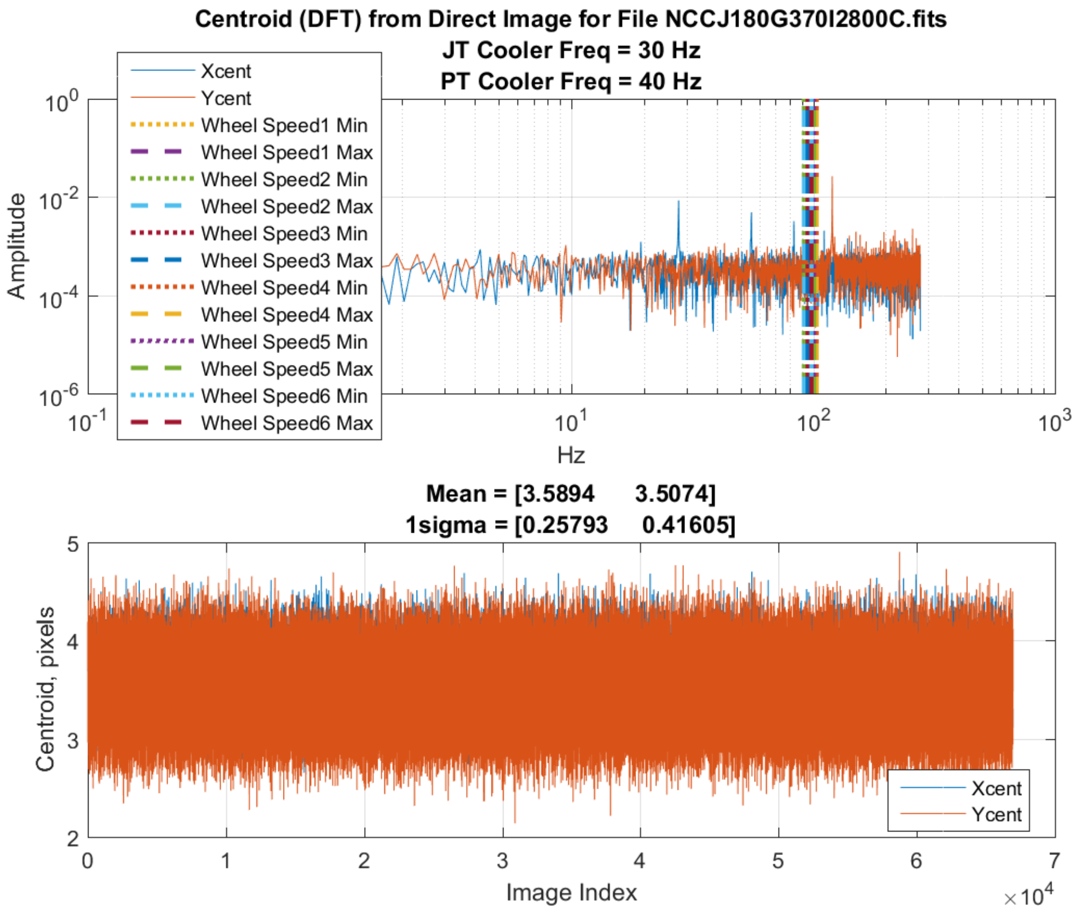

Figure 1. Example of NGAS tool "centroids_direct" plot

The “energy_<fn>” plots the total energy (no bias/background subtraction) in the 8x8 px subarray for each frame, as well as its PSD; this is useful to assess whether light is being lost during the course of the exposure, e.g., due to the target being placed too near the subarray edge.

Other plots show the values of the CC operational parameters, including the CC vibration measurements, and the RWA speeds over the time interval extracted from telemetry.

A selection of the operating parameters and the centroid results are logged in the CCJ_Output.csv file. It is suggested that a running log be maintained by appending this file to previous results, to facilitate trending.

3.2 IDL TOOL (*JITA*) ANALYSIS

The ***jita*** tool is invoked, in an IDL session, with:

IDL>jita, <*dir_name*> (if <*dir_name*> is not supplied, use the resulting pickfile dialog to select the directory)

There are many options available on the command line, for non-default behavior:

IDL> jita, [dirn, [logfn=logfn, ana=ana, movie=movie, no_show=no_show, sfmt=sfmt, mkplt=mkplt,
no_fof=no_fof, satin=satin, freq=freq, pkthresh=pkth, xfreq=xfreq, yfreq=yfreq, pdf=pdf, ql=ql,
zip=zip, term=term]]]

where:

dirn directory in which the fits file (uncalibrated, level 1 processed NIRCam 8x8 px time series observation) and engineering telemetry FOF (.csv) file are contained; output is also written to this directory

logfn name of the output csv log file (default 'jitlog') to which selected results will be appended

ana PSF center finding algorithm (default is 2D Gaussian fit 'g', can also use faster, but less accurate for very small offsets cross-correlation 'x', or centroid 'c')

movie make an avi file movie of the first n time series frames: movie=n (default is 0, no movie)

no_show do not display the results to screen; NOTE: this option caused corruption of pdf output on plwss2 during LRE4

sfmt format of the output plots (default is .png; set to null string '' for no plots saved)

mkplot select which plots to make (default is all). See below for list of plots (Boolean array of size 10)

no_fof do not prompt for, or use, engineering telemetry FOF file

satin frame (group) number at which saturation begins to occur (default=0, no saturation)

freq set to use previously computed time series results to perform additional frequency analyses

pkthresh specify PSD level above which frequency peaks are identified for each PSD type: [LOS_X, LOS_Y, Asym0, Asym45, Blur, EE]

x/yfreq frequencies and their halfwidths to mask for residual X or Y LOS jitter analysis: [f,hw] pairs in a 2xn floating point array

pdf set to write all output plots to a single pdf file (overrides smft keyword) and specify non-default output filename

ql set to perform only the initial quick look of data quality, such as checking for saturation, and to make an initial estimate of the RMS jitter; only the data quality plots (Fig 1) are generated.

zip set to create a zip file of the pdf plots, the csv file of offsets vs elapsed time, the csv file of PSD results and the updated jitlog.csv log file for dissemination to interested parties.

term set to print messages to the terminal, rather than to the jita_messages_log.txt file; if not set the plot windows will be deleted automatically upon jita completion, to enable automatic mode processing.

The tool produces many output products, listed briefly in Table 1, which may be selectively omitted using the *mkplot* parameter.

Table 2. Plots produced by the jita tool

Name	Index	Description
<fn>_pvi	0	Peak signal in each frame up the ramp, over-plotted for INTs
<fn>_evf	0	Total signal in each difference frame
<fn>_img	1	Median PSF from final (unsaturated) frame of all INTs
<fn>_?_ovt	2	Relative image offsets in X and Y vs. time for all difference frames
<fn>_?_ball	2	LOS jitter ball, with measured RMS
<fn>_?_avt	3	PSF asymmetry metric vs. time for all difference frames
<fn>_?_svt	3	PSF focus softness metric vs. time for all difference frames
<fn>_?_evt	4	Encircled and ensquared energy vs. time for all difference frames
<fn>_?_psd	5	LOS power spectrum indicating dominant frequencies in X and Y and marking RWA speeds and JT and PT frequencies
<fn>_?_ppd	5	LOS power vs log period in X and Y to emphasize low frequency components
<fn>_?_psa	6	PSF asymmetry metric power spectrum indicating dominant frequencies in X and Y and marking RWA speeds and JT and PT frequencies
<fn>_?_pss	6	PSF (focus) softness power spectrum indicating dominant frequencies in X and Y and marking RWA speeds and JT and PT frequencies
<fn>_?_pse	7	EE power spectrum indicating dominant frequencies in X and Y and marking RWA speeds and JT and PT frequencies
<fn>_?_Xwave<n>	8	Waveform of LOS X offsets at one of n specified frequencies
<fn>_?_Ywave<n>	8	Waveform of LOS Y offsets at one of n specified frequencies
<fn>_?_ballfilt	9	Jitter ball, with measured RMS, after removing specified LOS frequencies

<fn> is the fits file rootname (e.g., jw00770001001_02102_00001_nrca3_uncal) and ? is the PSF centroiding technique: ‘x’ for cross-correlation (default), ‘g’ for 2D gaussian fit, ‘c’ for combo-centroid.

The number following each plot identifier is the index of the Boolean array mkplot, which may be used to specify which plots to make (1) and which to skip (0). The default is to produce all plots. For example, mkplot=[0,0,0,0,0,1,0,0,0,0] or [0,0,0,0,0,1] produces only the LOS PSD plot, and specifying mkplot=[1,1] will yield only the initial data quality plots.

Refer to “IDL Jitter Assessment Tool (jita) User’s Guide”, rev C, for a more complete description of the tool’s usage and output products.

3.3 JITA NOISE FLOOR ESTIMATION

Measurement noise is a significant contributor to these short exposure, rapid readout subarray jitter determinations. An IDL program (jitsim.pro) was developed to quantify the noise and sensitivity as a function of the adjustable exposure parameters: number of groups (frames) read out between resets, number of integrations per exposure and signal level in the PSF of each difference frame. The latter is determined solely by the combination of target brightness, NIRCam filter and the non-adjustable rapid read cadence of the 8x8 subarray (2.2ms). The Fine Phasing APT template was updated in 2020 to permit selection of a few filters (F212N, F210M and F200W) to alleviate the initially restrictive implementation.

Simulations were performed using a rapid-read dark exposure obtained in the ISIM CV3 campaign to demonstrate the use of the 8x8 subarray for jitter measurement purposes. To these frames were added simulated, monochromatic (2.0 um) PSFs created with a WFE map representative of the OTE+NIRCam and with Poisson noise added. The PSFs were further aberrated with tip/tilt (to simulate random and sinusoidal LOS jitter) and sinusoidal focus and astigmatism terms (to simulate potential figure vibration).

The resultant image sequences were formatted as per the DMS pipeline and written to fits files for evaluation by the jitter measurement tools. These studies informed the selection of target and exposure parameters used for the flight measurements and provided confidence that LOS jitter measurements of order 1 mas could be accurately made and any significant underlying periodic oscillations (within the bandwidth of the observations) correctly identified.

Because the JWST flight LOS jitter performance has been found to be excellent, at approximately 1 mas rms, radial, these measurements are significantly affected by the measurement noise. The underlying true jitter may be estimated, assuming the noise and the jitter oscillations are uncorrelated, by “de-RSS-ing” the noise level expected for a given measurement. To that end, a series of simulations were performed with differing signal levels comparable to the range of signals seen in the jitter measurements using various targets, to date. The results were fit with a 2nd order polynomial, as shown in Figure 2. This calibration was then used to compute the underlying jitter for each measurement, reported as “reduced” jitter by the ***jita*** tool.

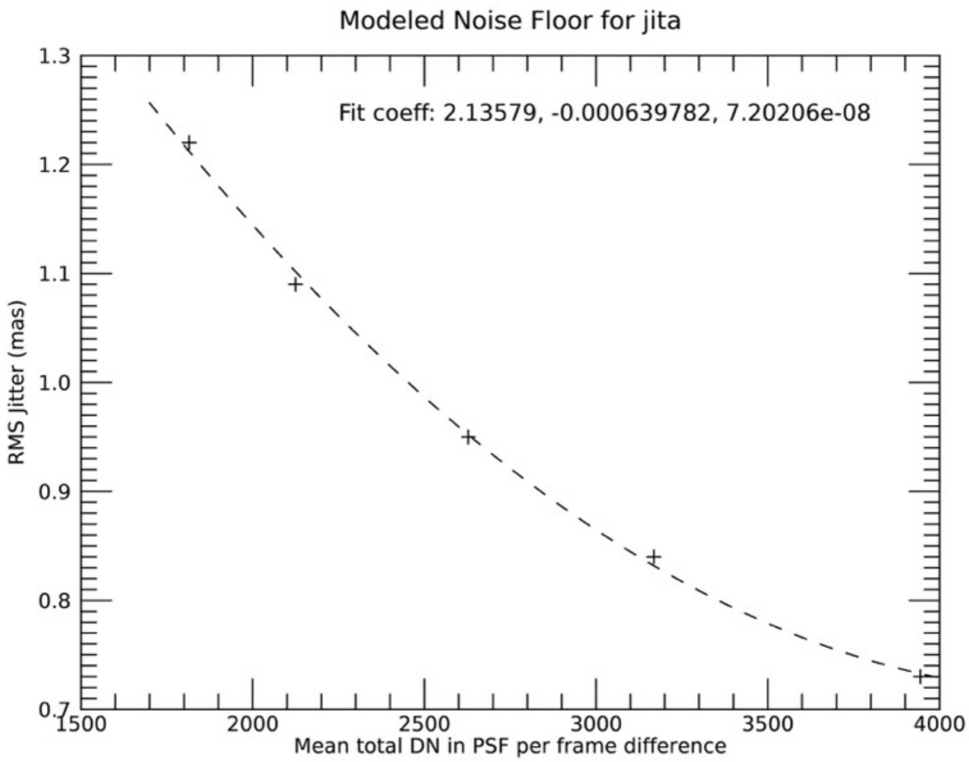

Figure 2. Modeled Noise Floor Estimate

3.4 ADDITIONAL FREQUENCY DOMAIN ANALYSIS

The ***jita*** tool permits determination of the RMS jitter after filtering specified frequencies, such as those attributed to the RWAs; the wheel rotation rate frequencies are indicated on the PSD plots. These (and their harmonics) that appear at/near PSD peaks are suspect and may be filtered to assess the residual jitter due to the CC alone, which is reported in the `*ballfilt` plot. By default, the most significant peaks in the ***jita*** tool PSD are removed and the RMS jitter recalculated (to assess how good the jitter would be without their presence), but the user may specify which frequencies to filter. When iterating/adjusting the filter frequencies the user may set the /freq keyword to use the previous basic centroiding analysis to speed up processing, e.g.:

IDL> jita, <dir_name>, /freq, xfr=[[56.2,1.2],[56.2*2,2.]]

This will use the image centroid information determined with a previous run of the tool, but filter frequencies around 56.2 +/- 1.2 Hz and its first harmonic from the X axis PSD, then recompute the RMS jitter in that axis.

The tool also computes and plots, in the `*Xwave`*n* and `*Ywave`*n* plots, the waveforms of identified peak frequencies, which may be useful in identifying their origin (sinusoidal, pulse-like).

3.5 PSF METRICS TO DETECT OSCILLATORY WFE

The ***jita*** tool also computes and performs frequency domain analysis on several PSF metrics: encircled and ensquared energy, and focus softness and asymmetry metrics. Their PSDs and identified peaks are shown in the *pse, *pss and *psa plots. These may be useful for identifying periodic variations in the WFE ("figure vibrate") and may be of use for studies of the observatory structural dynamics.

Simulations have demonstrated that oscillatory WFE in the form of focus and astigmatism can be detected in the blur and asymmetry metric PSDs, respectively, at the level of a few nm RMS. Figure 3 shows the asymmetry PSD from such a simulation test, in which astigmatism was imposed at 120 (0 deg) and 100 (45 deg) Hz with amplitude of 10 nm and 5 nm RMS, as well as defocus at 70 Hz with amplitude of 10 nm RMS, in addition to random LOS jitter. These oscillations are all readily detected.

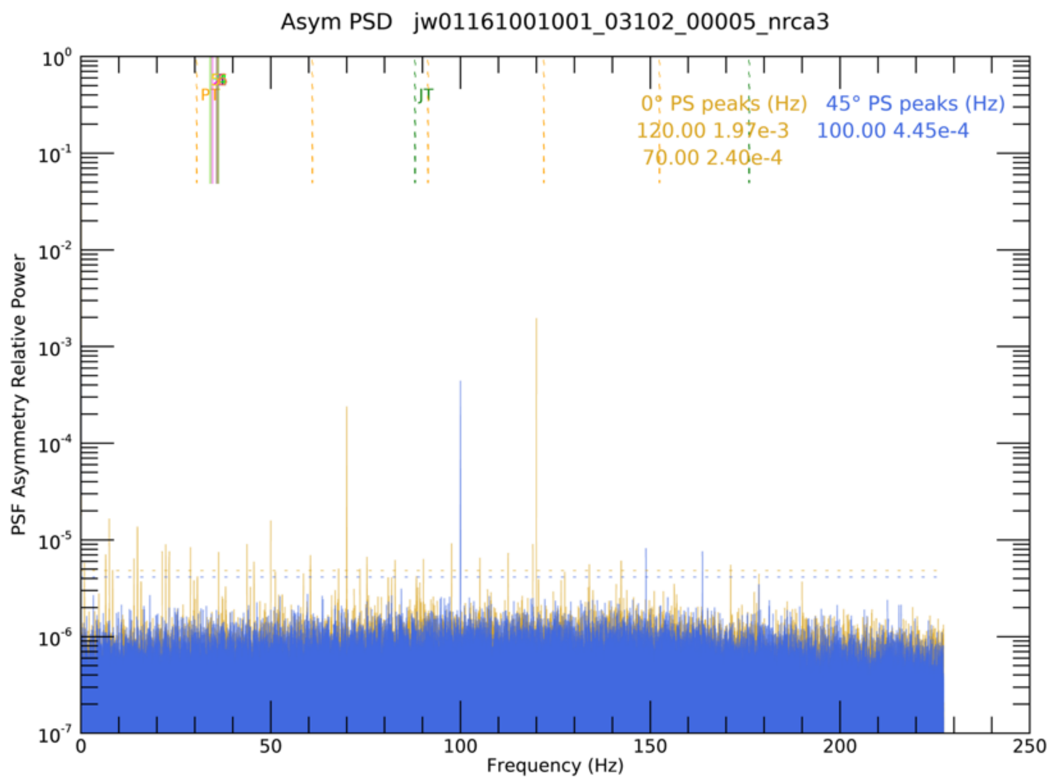

Figure 3. Asymmetry metric PSD of simulation showing sensitivity to periodic astigmatism

In practice, throughout the commissioning measurements, only one PSF asymmetry feature has been persistent, at ~ 120.1 Hz, coincident with a feature in the LOS PSD at the same frequency (Fig 4). This has been ascribed to a rocking mode of the SM, potentially being excited by the PT compressor (4^{th} harmonic of 30.4878 Hz drive frequency) but has diminished in intensity in later observations though the drive frequency has not changed.

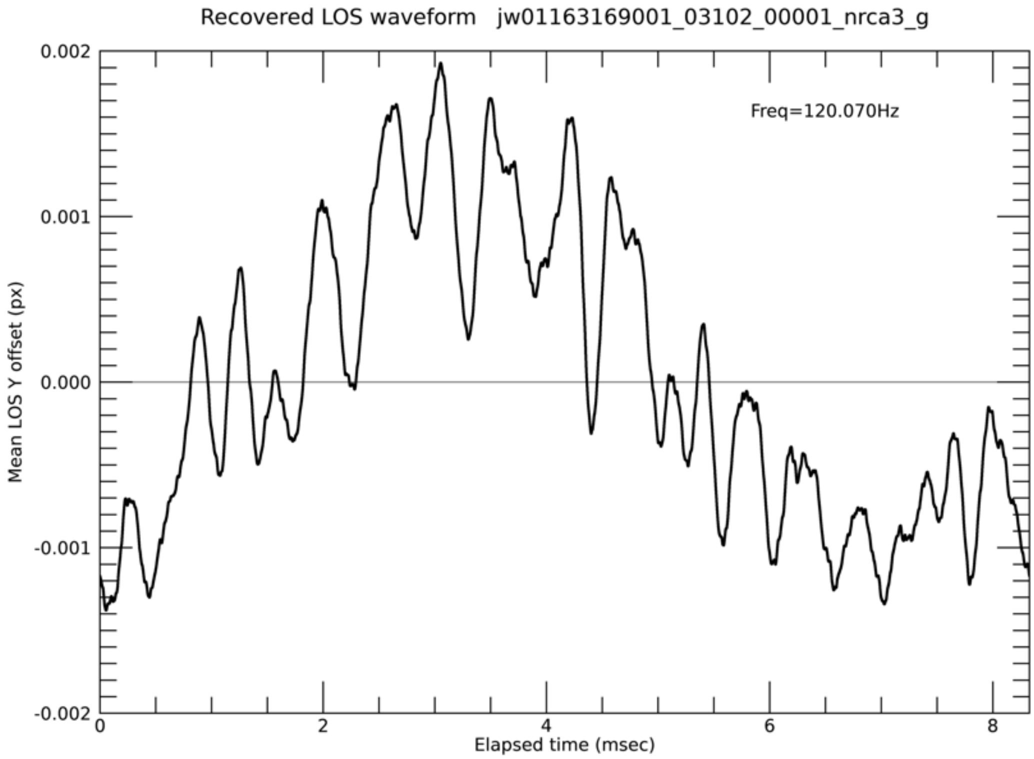

Figure 4. LOS Y axis waveform at 120.1 Hz

The features seen in the PSF Blur PSD at 7.44 Hz and harmonics, or 6.22 Hz and harmonics in later observations obtained with 72 groups, are correlated with the exposure parameters and due to detector ("brighter-fatter") effects, not periodicity in the optical PSF properties.

4.0 CRYO-COOLER EFFECTS

One of the major drivers of the jitter measurement program is to assess the effects that the MIRI cryo-cooler (CC) has on the LOS jitter, since it is comprised of two mechanical compressors which, though designed to produce minimal vibration, might nevertheless excite certain Spacecraft or OTE modes that could increase the observed jitter.

Refer to the Commissioning Analysis Plan (JWST-STScI-007225 Rev B) and the documents referenced therein for a more detailed description of the planned CC-induced jitter evaluation process.

4.1 STATE TRANSITIONS

Two specific measurements were included in the baseline commissioning plan; the first (CAR-803, PID 1161, OPT-24) when the CC was initially transitioned from State 3 to State 4, increasing power to the compressors, and the second (CAR-804, PID 1170, OPT-33) after the CC achieved steady state thermal performance (State 6). Neither indicated a significant involvement of the CC with LOS jitter.

An optional frequency sweep was included in CAR-803, in case the jitter was found to be significantly affected by the transition from State 3 to State 4. This included jitter measurements after 4 additional pre-selected PT frequencies were commanded, to attempt to find a “quieter” PT operating frequency. This contingency was not required when the measured jitter at the nominal PT frequency was found to be < 1.5 mas rms (radial) and no indications of significant CC effects were seen in the frequency analysis.

An additional frequency sweep was planned (CAR-805) after reaching State 6, to assure that the PT frequency was not on an edge of the observatory response such that small drift of the PT frequency might excite a mode that would degrade jitter performance. Although that sweep (4 commanded frequencies, with two adjacent frequencies both above and below the nominal) was not planned as a contingency, the excellent LOS jitter performance measured to date, with no indication of a significant CC effect, convinced the Project to dispense with that portion of the plan. CAR-805 was not executed. The CC PT and JT frequencies have not been changed from their initial settings as of this writing, although their drive levels have, of course, varied through the initial cool-down and during detector anneal cycles.

4.2 JT-ASSISTED ANNEAL

Another CC-related jitter measurement program (CAR-905, PID 1439, MIR-81) was executed on 13 Apr 2022 to discern any effect of the CC on jitter when the JT-assisted detector anneal was initially performed. This test collected 27 consecutive exposures, each 4 minutes long with 1800 integrations, to cover the ~ 2hr test period during which the JT and PT drive levels were changed to perform a rapid anneal and recovery. Each exposure was separately measured with the ***jita*** tool to determine the jitter magnitude and look for frequency signatures that might be associated with the CC. No correlation between CC drive levels and jitter performance was detected (Fig. 5), nor was any new PSD feature identified.

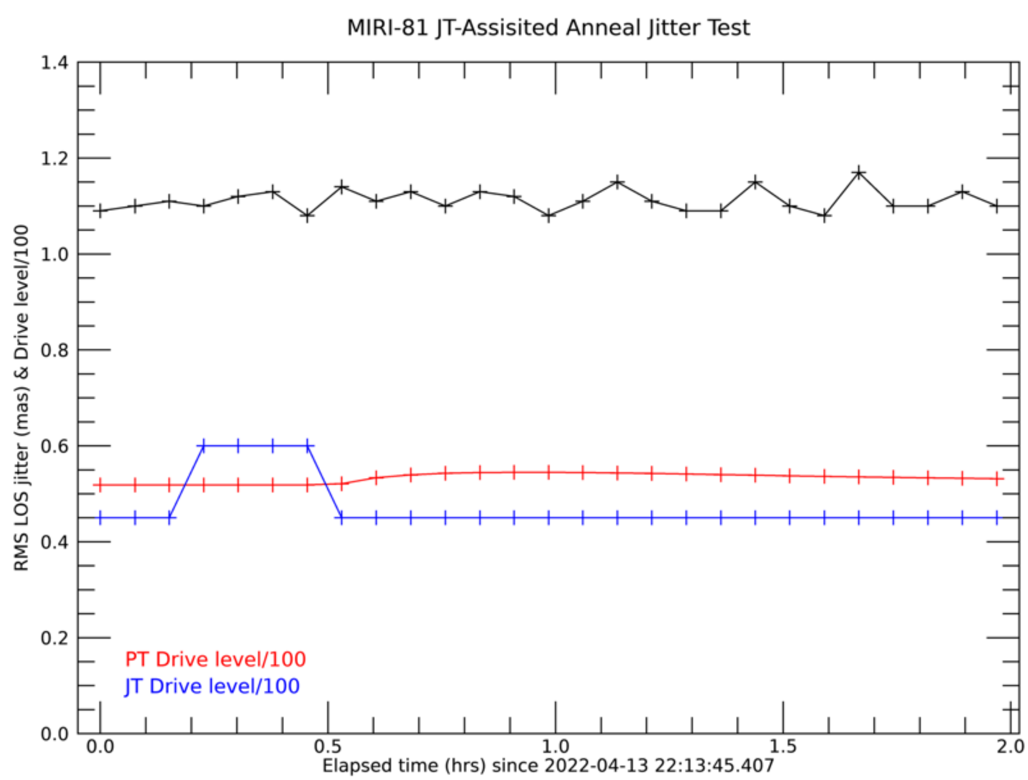

Figure 5. MIRI JT-assisted anneal jitter test results

5.0 MEASUREMENTS & RESULTS

Results of all of the LOS jitter measurements, from the initial investigation during CC transitions through the Cy-1 monitoring, were communicated to a large list of interested parties and meetings were held to discuss the early results and paths forward. The list of notification recipients is shown in Appendix A. Results were also presented regularly at the JDB forum and continue to be included in the JWB meetings.

A log of all jitter measurements made as of this writing is presented in Appendix B, extracted from the jitlog.csv output product of the ***jita*** tool. The columns list the date/time and MJD of the observations, the science data fits filename, telemetry FOF filename, the offset determination analysis technique (g for 2D gaussian fitting) and exposure parameters, NGROUPS/NINTS. Next are LOS jitter analysis results: the X- and Y-axis RMS image offsets (px) and conversion to RMS radial offset in mas, then the reduced (measurement noise contribution removed) jitter, also in mas (radial). These are followed by the 6 RWA speeds in Hz, then the CC JT and PT compressor frequencies and their respective drive levels telemetered during the jitter measurement interval.

5.1 THE OTE WAVEFRONT MAINTENANCE AND JITTER MONITOR PROGRAM

Beginning shortly after the OTE alignment has progressed to the fine phasing at the NIRCam fiducial field point, the CAR71.n (OTE-26, PID 1163) was used to assess the LOS jitter. The first instance of this program made the initial, successful attempt to use the onboard target acquisition script to place the target at the center of the 8x8 subarray. The LOS jitter was measured at 1.04 mas rms (radial), including the measurement noise contribution. This was deemed excellent, permitting the continuation of the commissioning program without further investigation.

The LOS jitter has been dominated by low frequency oscillations, predominantly at ~0.3 and 0.04 Hz through the commissioning period and beyond. This can readily be seen in the PSF offset vs. time plots; an example is shown in Fig 6. It is further apparent in the PSD vs. period plots as demonstrated in Fig 7.

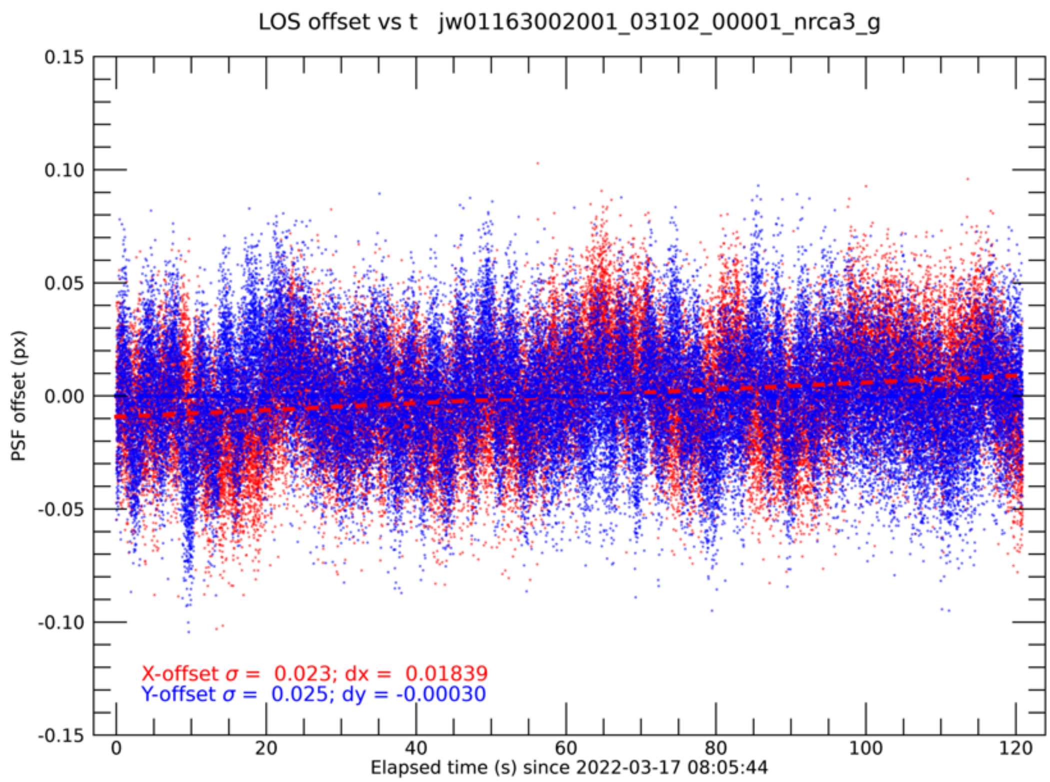

Figure 6. PSF position offsets vs time for initial jitter measurement

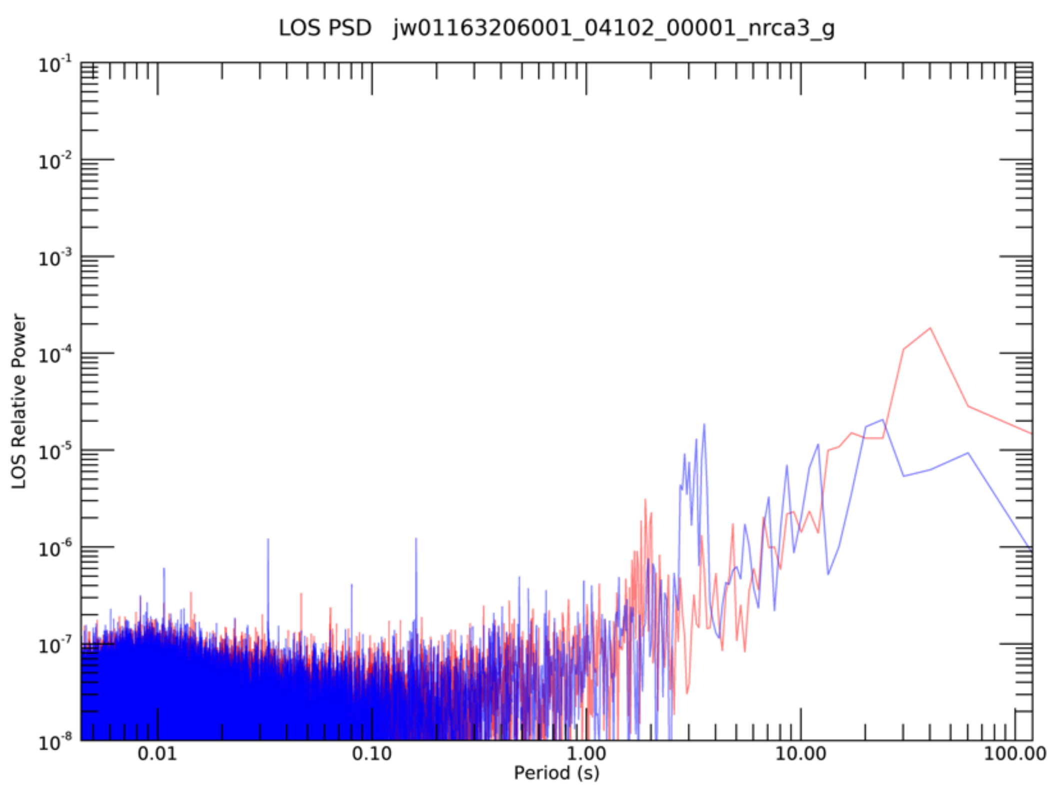

Figure 7. LOS PSD vs period showing low frequency disturbances

Since the initial measurements, the CAR 71.n program has been exercised ~45 times, in later stages at approximately 2-day cadence, in conjunction with the WF maintenance fine phasing measurements (and occasional WF control mirror moves, as required). Targets were selected from a list generated by Tracy Beck that covers the entire sky with K~9, isolated stars. The same observing parameters (F210M, ngroups=60, nints=900) for all but the final few instances, at which point brighter targets (K~7) were selected from a similar list, since the fine phasing (FP) measurements had transitioned to using only the PM8 weak lenses, for which the brighter targets were viable and preferred to minimize exposure times. Although this change was made for efficiency of the FP WF measurements, it impacts the LOS jitter exposures as well since the same target is used for both (for efficiency) and to better center the target for the FP exposures which immediately follow the LOS measurement. This required a change to the exposure parameters to use the F212N filter, with ngroups=72, nints=750 (and, for the TA, ngroups=3).

The jitter measurement noise contribution was found to increase significantly with the use of the F212N and K~7 targets, compared to that seen in the earlier F210M, K~9 measurements, due to lower signal levels in each frame. Efforts have been made to discern the underlying jitter magnitude by removing the noise contribution (ref sec 3.3).

5.2 THE CYCLE-1 CALIBRATION PROGRAM

After OTE commissioning was completed and the final instance of CAR 71.n executed on 27 June 2022, the jitter monitoring continued in the Cycle 1 calibration program, again as part of the 2-day cadence WF maintenance program. This was implemented in APT as PIDs 2586, 2724, 2725, and 2726, each of which covers a quarter of the sky with 100 targets selected for magnitude (K~7) and isolation. These target sets provide coverage within ~ 5 degrees of any point. Five observations are included for each target, so targets may be used repeatedly without any modification to the APT. In practice, the target for any given WF maintenance observation is selected by PPS from the 4 programs to be close to the path that the slew would follow between the preceding and subsequent observations, thereby minimizing the slew time overhead.

It is expected that in the future the LOS measurements may be dropped from the WF maintenance program, perhaps later in the Cy-1 program, when they are deemed less important (jitter stability has been well established) in the interest of efficiency.

5.3 AUTO-RUN ANALYSES

The ***jita*** program has been adapted to run automatically upon receipt of science data and FOF telemetry reports on the WSS workstation, sending an email with results (sample shown below) to the TEL_WFSC distribution. The data package produced by ***jita*** for each observation will also be archived and available in the WSSTAS system.

Correction Id:
    R202208180B

Calibrated Science Data:
    /internal/2/WEx_Cache_Ops/data/prop02725/visit389001/images/jw02725389001_04102_00001_nrca3_uncal.fits

Calibrated Engineering Data:
    /internal/2/WEx_Cache_Ops/engineeringData/2022-08-18/FOFWSS2022230152121919.CSV

Total RMS Jitter (unfiltered):

Unfiltered RMS jitter in X, Y (px): 0.038, 0.038; RSS (mas): 1.68

Reduced Jitter in (mas): 1.03526

6.0 ARTIFACTS AND ANOMALIES

Several anomalous jitter measurements have occurred during the commissioning period that demanded investigation and explanation.

PID 1162 Obs 009, 24Mar2022 – An abnormal level of power appeared in the EE PSD (Fig. 8) with 17.2s periodicity and sawtooth waveform (Fig. 9). This is due to a detector effect, whereby charge is built up and then dissipated on the edge of the 8x8 subarray, most notably when the PSF is poorly formed, as it was for this exposure, placing significant signal levels beyond the edge of the 8x8 subarray, which bleed into the array. This strongly affects the EE calculation which uses the edge pixels for normalization. Per John Stansberry, the rolling reset program used for this subarray takes 128 INTs to reset the entire detector, which, for our exposure parameters, results in a reset every 17.2 s, matching the periodicity that we measure in the EE. As long as the PSF is well maintained, this artifact is not expected to recur.

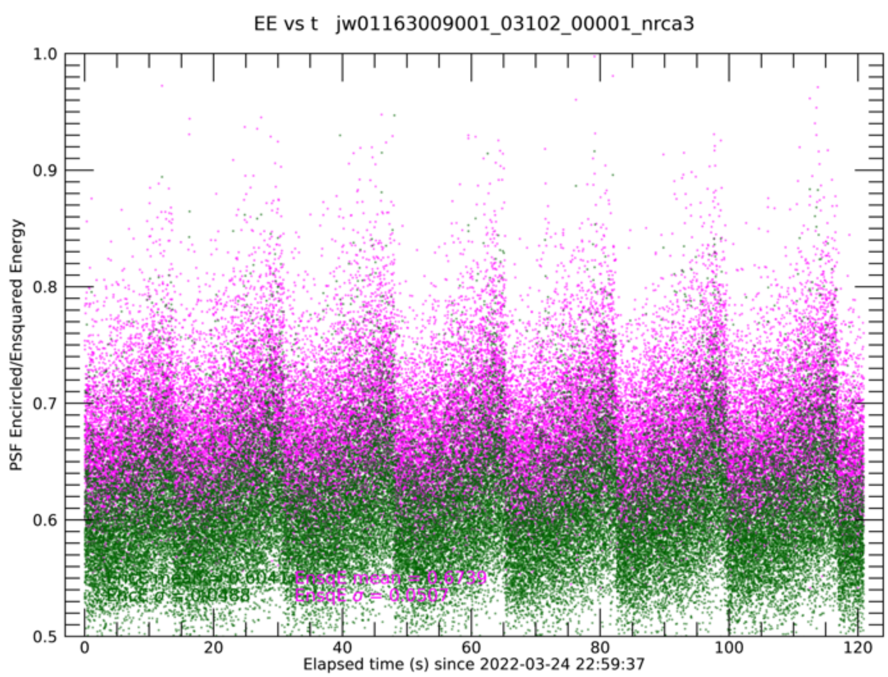

Figure 8. Encircled Energy vs time with poorly formed PSF

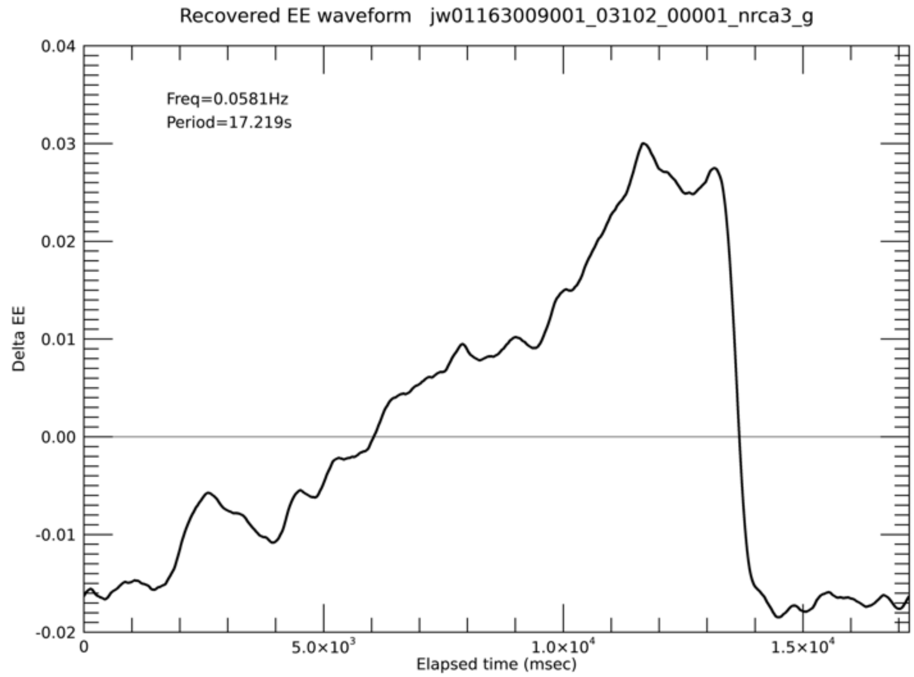

Figure 9. EE waveform showing reset anomaly

PID 1170 Obs 1 Exp 2, 12Apr2022 – This 2nd of 5 identical exposures, obtained as part of the CC jitter investigation after reaching thermal steady state, exhibited a large image offset excursion (Fig. 10) resulting in an anomalous LOS jitter evaluation (>6 mas). This was determined to be due to an HGA gimbal move during the jitter measurement.

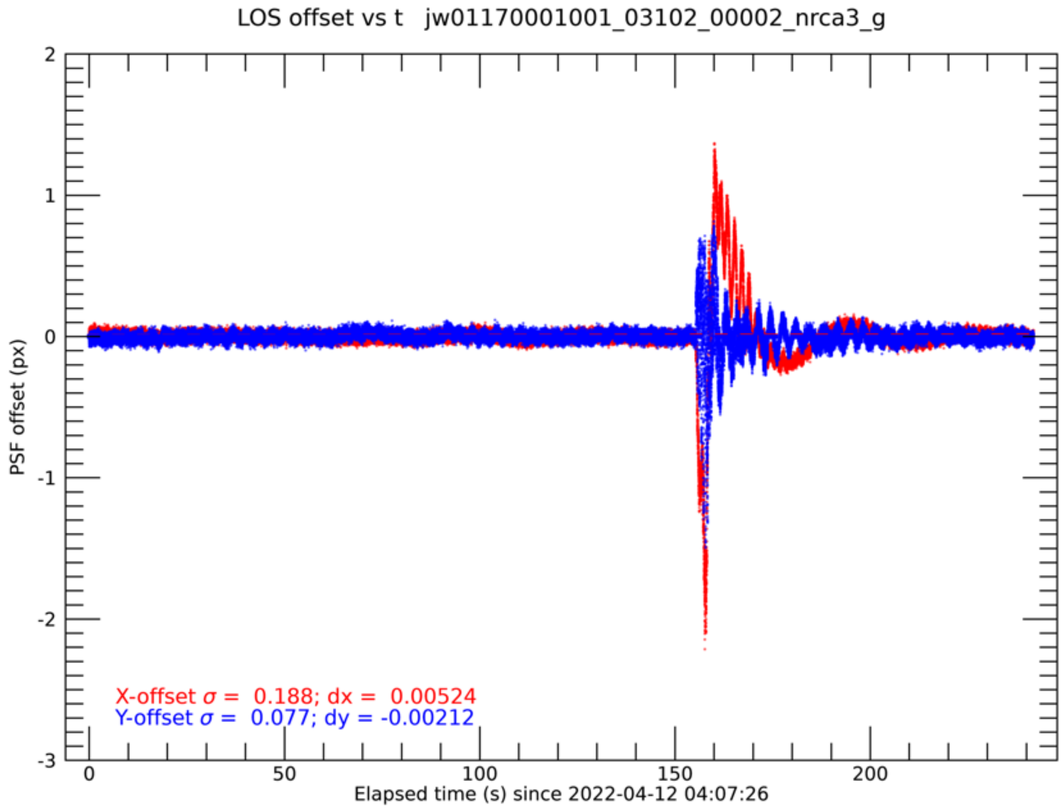

Figure 10. PSF position offsets sensed during a HGA move

PID 1163 Obs 60 28May2022 – No target was present in the 8x8 subarray, although the TA was "successful", permitting the observation to continue. This turned out to be due to a GS catalog error, which placed the target images ~ 1.5 arcsec from the intended location. Nevertheless, the TA algorithm must have found something in its 64x64 image and the observation progressed, with the WF sensing images displaced from their nominal locations by ~ 50 px. The ensuing 1163 Obs 61 measurement of the same target, scheduled less than a day later, unfortunately used the same GS configuration and failed this time at the TA stage, so the observations were lost.

PID 2586 Obs 67 20Aug2022 – The LOS jitter was much larger than normal, >3 mas, asymmetric with most of the disturbance in the Y (V3) axis (Fig. 11) and an atypical PSD with increased power at frequencies < a few Hz. This was traced by the guider team to the use of a double star for the guide star (catalog issue), which was causing the FGS centroids to oscillate between the two stars (Fig 11, right, courtesy A. Marrione). The CC drive levels were also seen to be atypical, but this was due to an unrelated issue, with the CC JT being in an attenuated mode due to an earlier vibration event and the PT drive increased to compensate. The CC vibration level telemetry was in family. The following jitter measurement, 2725:485 on 22 Aug, showed jitter and CC drive levels to be back in family.

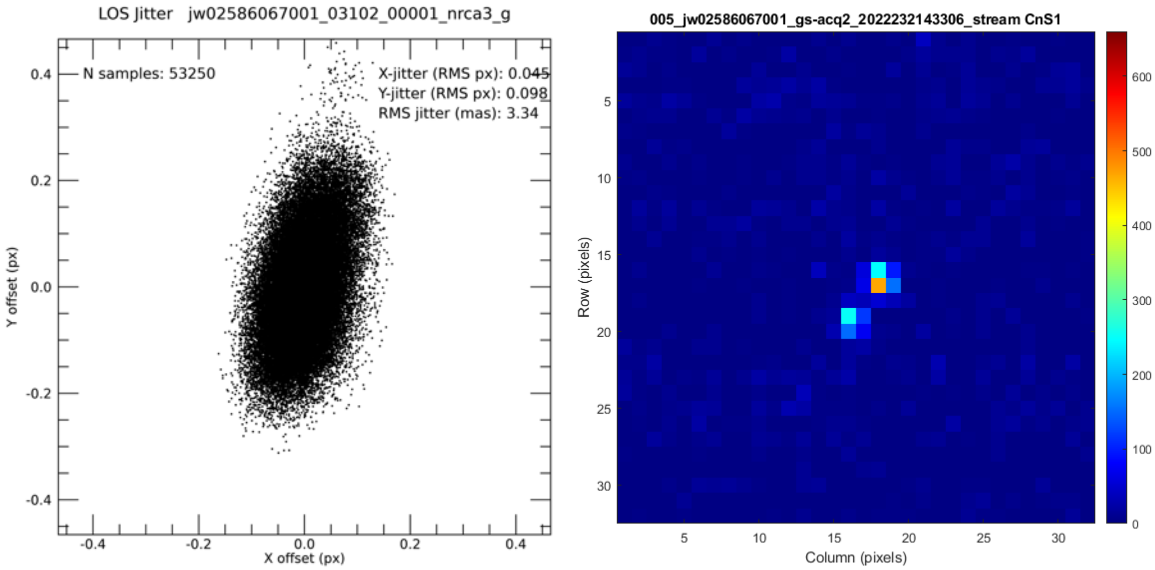

Figure 11. Anomalous jitter (left) and double GS cause (right) for observation 2586:67

7.0 <u>TRENDING</u>

The behavior of the LOS jitter has been showing indications of evolution. Although no cause has been identified, and the magnitude of the jitter remains well below specifications, some changes have occurred through the first ~ 6 months of measurement.

After transitioning to the F212N filter and K~7 targets for the Cy1 measurements, the noise contribution has clearly increased due to lower PSF signal per frame and must be accounted for in trending studies. Model simulations were used to calibrate the expected noise floor depending on the signal level of the PSF and then used to remove that contribution (de-RSS, assuming no correlation between noise and LOS signal). The resulting underlying jitter value is reported in the ***jita*** products as “reduced” RMS jitter (see sec 3.3), and plotted in Fig. 12 (green), with median value of ~ 0.8 mas.

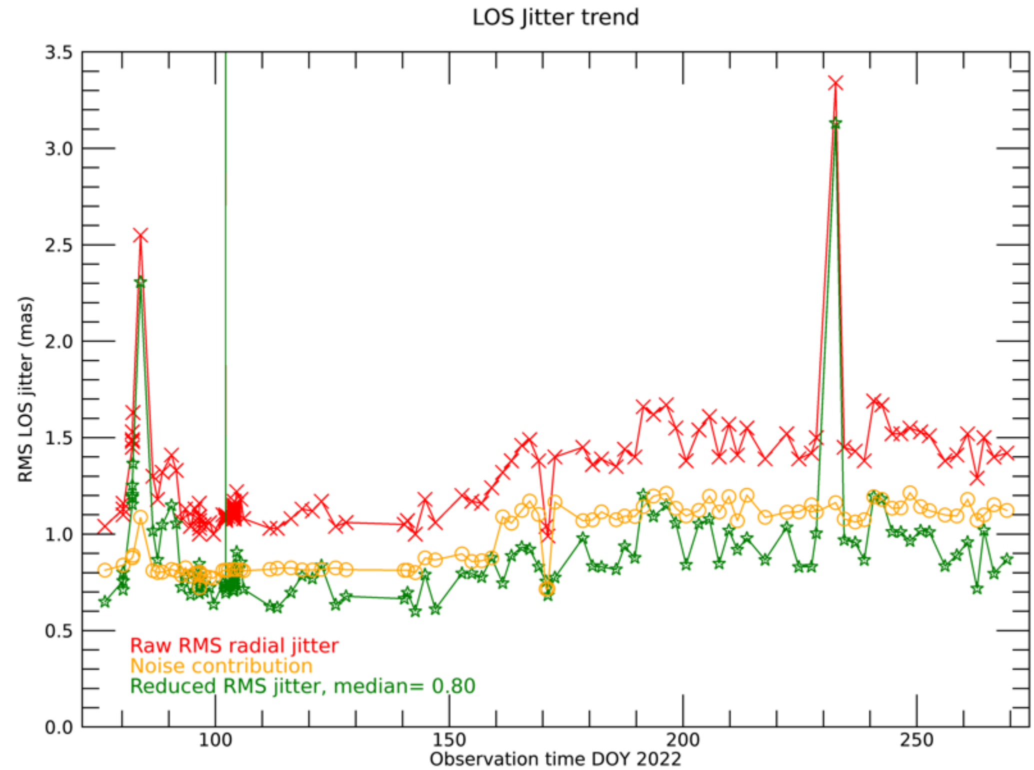

Figure 12. LOS jitter measurements

A peak at ~120.1 Hz is a staple feature in the early LOS PSD plots, particularly in the detector Y or V3 direction, and also appears in the PSF asymmetry metric PSD. This was conjectured as being due to a rocking mode of the SM, but its stimulation source is unclear, perhaps due to the 4th harmonic of the CC PT compressor frequency, although the frequencies do not exactly match. The waveform is nearly sinusoidal with an amplitude of ~ 0.001 px, so contributes negligibly to the LOS jitter (sec 3.5, Fig. 4). However, this feature has recently been much less prominent though the PT frequency has not changed.

After accounting for the noise contribution, there are some periods of increased jitter seen in the recent data. These generally occur in measurements with relatively large very low frequency (< 0.1 Hz) disturbances, which have been attributed to fuel slosh, with additional contributions due to disturbances near 0.3 Hz, which have been attributed to bending modes at the 1 Hz isolator at the SC/OTE interface. These modes dominate the LOS jitter and are readily apparent in the image offset vs. time plots produced by ***jita***. No clear correlation between the amplitude of the fuel slosh modes and duration of the slew to target has been apparent over the typical slew range of ~ 5 to 150 deg. Figure 13 shows the history of the ~0.04 Hz disturbance levels, which vary in power by an order of magnitude and direction, although the X axis (along V3) is dominant.

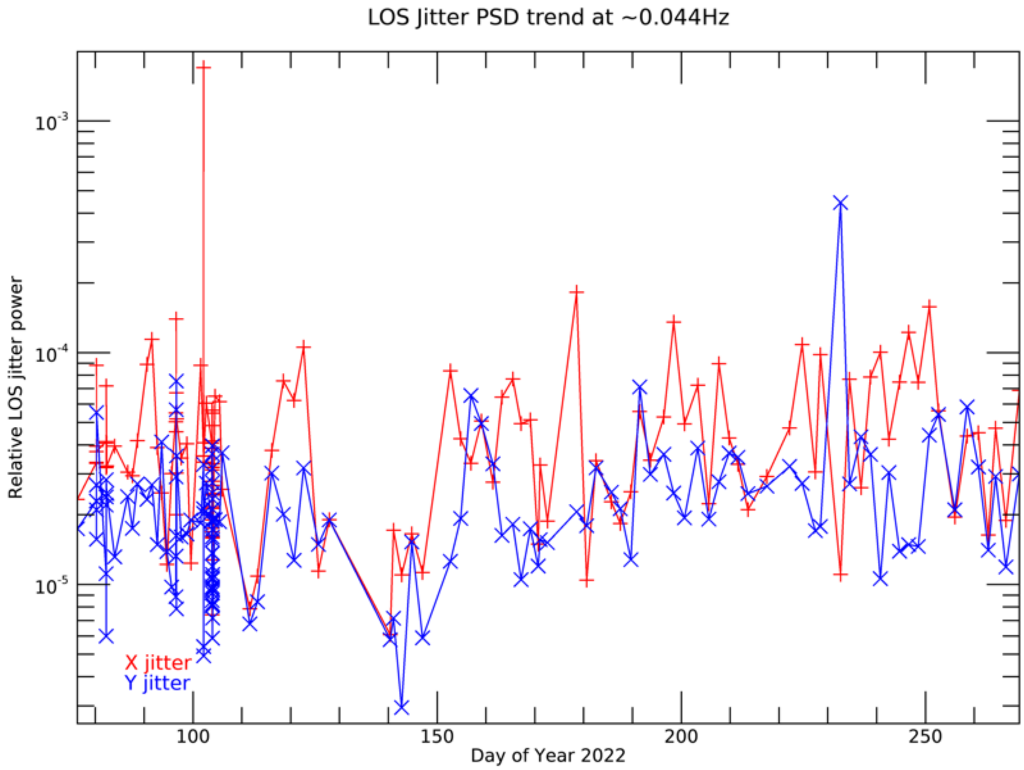

Figure 13. Relative power of ~0.04 Hz LOS disturbances

Throughout the commissioning period, no clear indications of a LOS response to the RWAs was noted. However, in July 2022 a series of Cy-1 measurements indicated that RWA6 may be causing minor LOS jitter at its fundamental frequency in the range 15-18 Hz, as seen in the PSD plots. This appears to be nearly sinusoidal with amplitude of ~ 0.1 mas in some measurements but strengthened considerably in the 10 Aug (DOY 222) data, at 16.25 Hz, predominantly in the Y (V3) axis as shown in Figures 14 and 15. This signal also appeared strongly in the PSF asymmetry metric PSD. Fig. 16 shows the LOS PSD power at the RWA6 frequency vs. that frequency for all of the jitter measurements to date; a resonance appears to be excited in the vicinity of 16-17 Hz. Only during the interval DOY 190-230 have any of the RWAs wandered into this frequency regime, as shown in Fig. 17. Also, on DOY 244, a relatively strong feature appeared in the Y axis LOS PSD at 30.18 Hz, again near the RWA6 frequency.

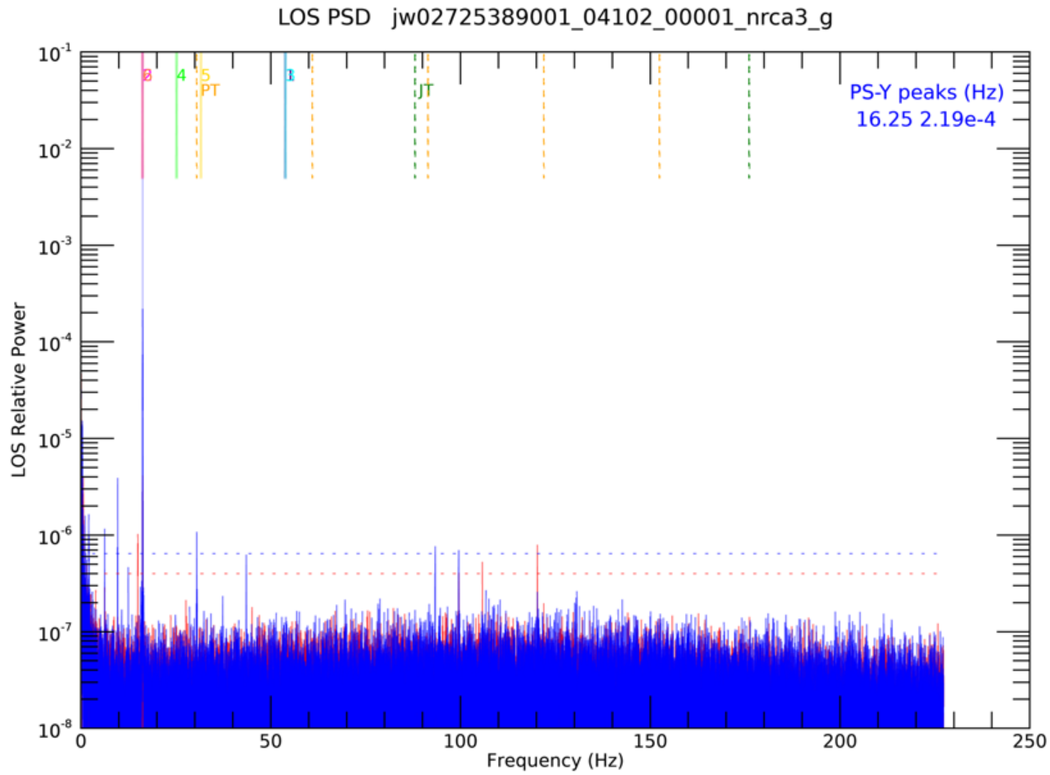

Figure 14. LOS PSD exhibiting large peak at 16.3 Hz coincident with RWA6 frequency

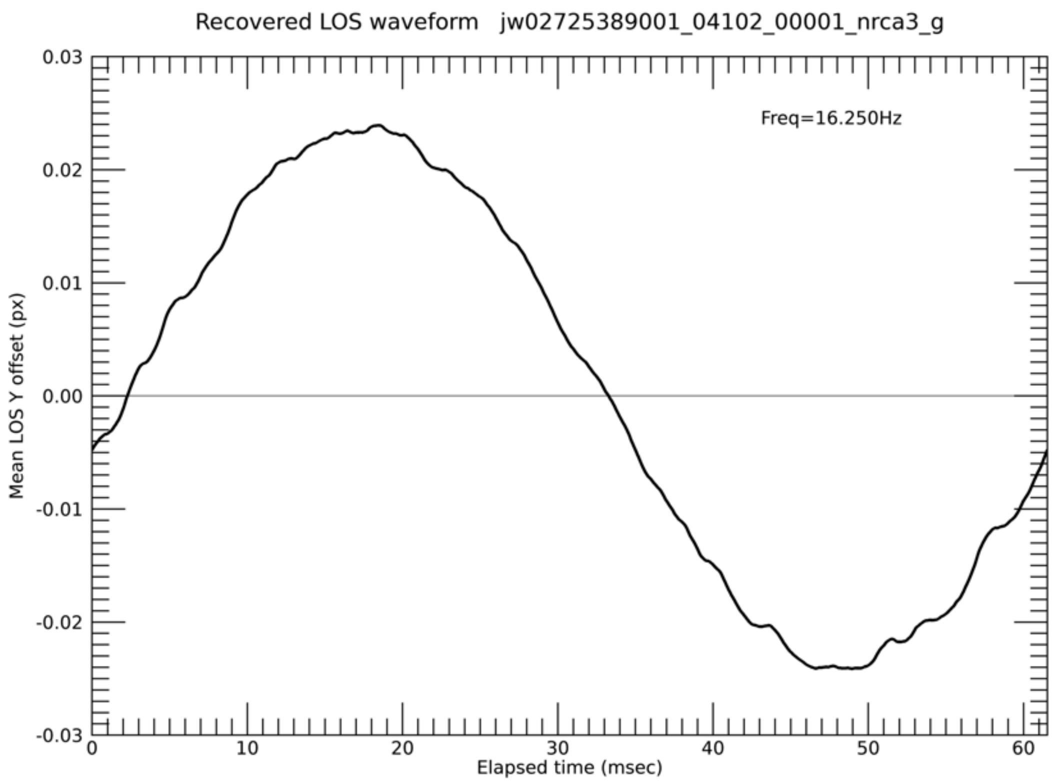

Figure 15. Waveform of 16.25 Hz LOS disturbance

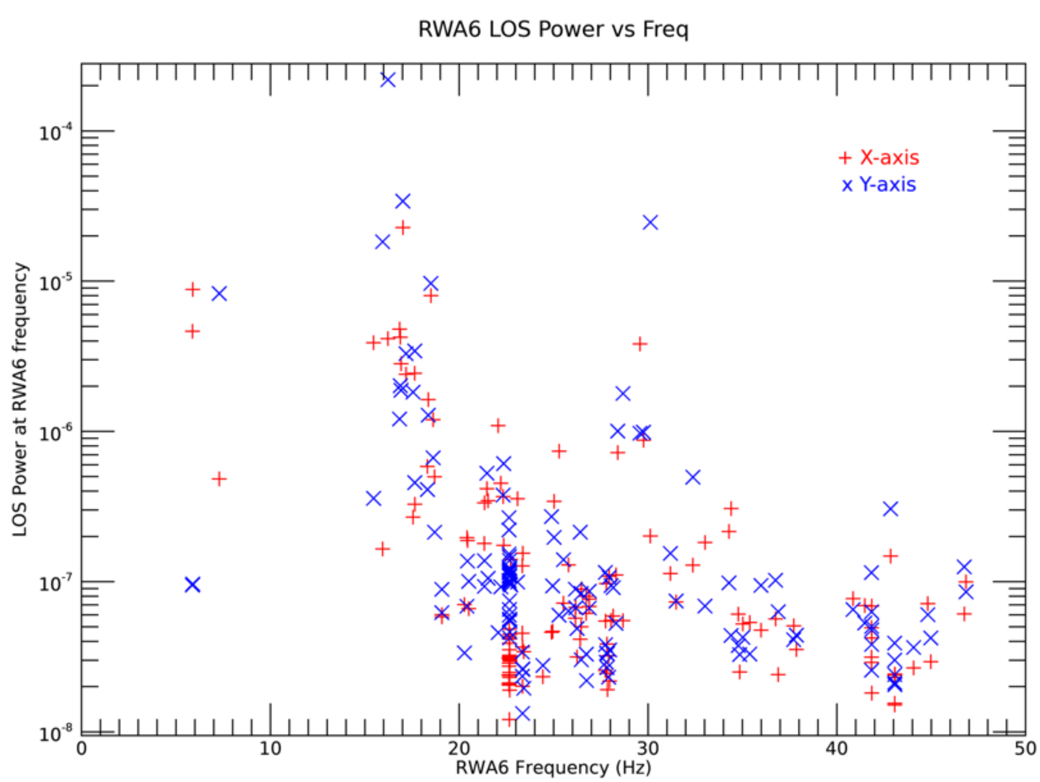

Figure 16. LOS PSD power at RWA6 frequencies

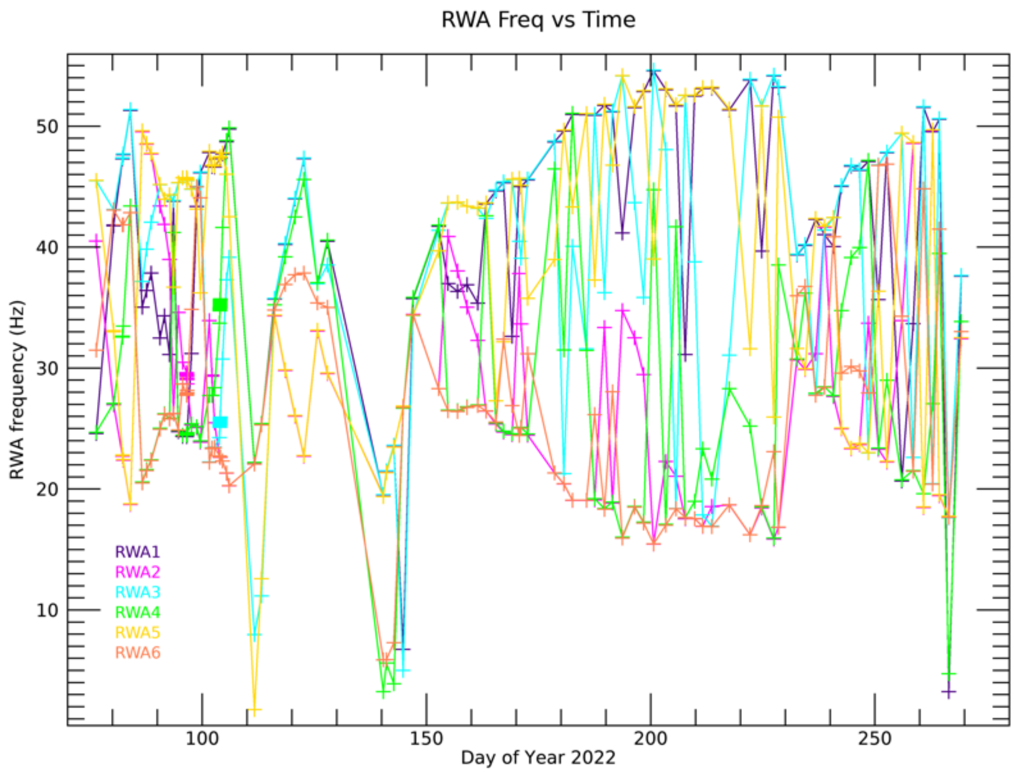

Figure 17. RWA frequencies during LOS jitter measurements

The guide star brightness can also have a significant effect on the measured LOS jitter. The guider NEA vs. fine guide counts is shown in Fig. 18, courtesy Begoña Vila, and indicates that for the faintest GS magnitudes (FGS ~18), corresponding to counts ~20,000, the NEA can dominate the jitter, with values > 2 mas. An example is PID 2586 Obs 282 on 28 Aug 2022 (DOY 240), for which the observed jitter was a relatively high 1.69 mas. The guider NEA was also quite high at (1.92,1.75) mas, with count rate of ~30,000, per the report (courtesy A. Marrione) found at https://www.fos.jwst.nasa.gov/edocs/display/FGSNIRISS/Week+of+22241 (NEA_Report_2022-08-29T14_03_42.csv). For the Cy-1 measurements no restrictions on GS magnitude have been levied, whereas during the commissioning period the GS magnitudes were limited to the range 12.4-16 by APT special requirement, so some higher jitter measurements should be expected when faint GSs are selected. Poorer guiding performance is evident in the LOS PSD plots as increased power in frequencies below several Hz. The GS magnitude can be found in the fits header and is reported in the jita_message_log.txt file.

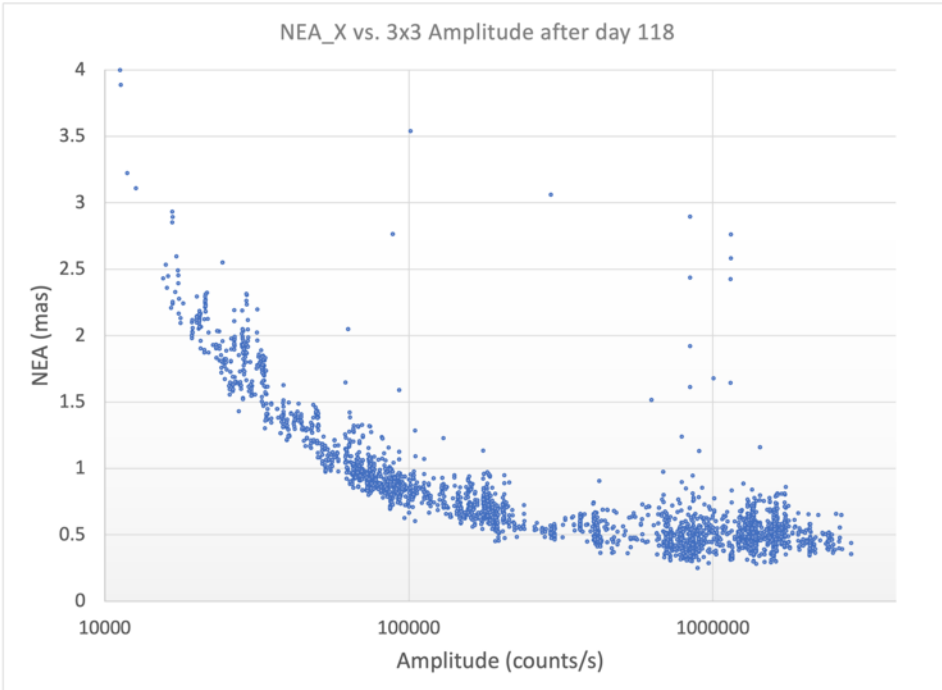

Figure 18. Guider NEA as function of counts in fine guide images

8.0 CONCLUSION

The LOS jitter measurement campaign during JWST commissioning has been successfully implemented. The on-orbit performance of the observatory has been demonstrated to be excellent, with the measured jitter readily beating the specifications and with little evidence of significant degradation from potential vibration sources, particularly the MIRI CC and the RWAs. The ACS, FSM and guiders are performing better than expected to deliver extremely stable images, with RMS jitter of ~ 1 mas, radial, to the SIs over their typical exposure intervals.

The LOS performance should continue to be trended, using the tools described herein, to assure on-going excellent performance and identify any issues as they arise, so they may be understood and potentially mitigated. Examples of out-of-family performance are described in Sec's 6 and 7, with explanations provided for the degraded jitter measurement. Future anomalous results should be investigated in similar fashion to attempt an understanding of root cause and possibly avoid or mitigate the degradation source. Some potential sources of change in the jitter performance are mechanical wear of the RWAs and CC compressors, changing degree of fuel slosh excitation as fuel levels decrease or ACS slew control parameters are modified and guider detector degradation.

9.0 REFERENCE DOCUMENTS

PIF OTE-24, -33	Proposal Implementation Form: *Cryo-Cooler Jitter Measurement (and Fine Tuning)*
JWST-STScI-005062	S&OC and OSS CryoCooler Tuning Operations Concept
JWST-PROC-042631, JWST-STScI-007197	JWST Wavefront Commissioning Procedure for OTE-24: Cryo-Cooler Jitter Measurements
JWST-PROC-042632, JWST-STScI-007196	JWST Wavefront Commissioning Procedure for OTE-33: Cryo-Cooler Jitter Measurements -2
JWST-STScI-007225 Rev B	WF Commissioning Analysis Plan for OTE-24 and -33: MIRI Cryo-Cooler Line-of-Sight Jitter Measurement and Tuning
https://jwstitarwiki.stsci.edu/display/WFSCOWG/Cryocooler+Jitter+Analysis+Tool	NGAS CCJ Tool How-to Use Description (B. Kulp)
NGAS Interoffice Memo 18-JWST-0024	JWST On-Orbit Cooler Jitter Evaluations and Tuning Tool Description and Users Guide (C. Rui and E. Caldwell, 12 Apr 2018)
https://jwstitarwiki.stsci.edu/download/attachments/17072565/jita_users_guide_rev_c.docx?version=1&modificationDate=1630594154994&api=v2	IDL Jitter Assessment Tool (jita) User's Guide, rev C (G. Hartig, 30 Jun 2021)
https://jwstitarwiki.stsci.edu/display/JWSTWWG/2019-05-21+Meeting+notes?preview=/81986824/81986825/PSF20Stability20Analysis20Tools.pptx	PSF Stability Analysis Tools, ppt presentation to WWG (G. Hartig, 21 May 2019)

10.0 ACRONYM LIST

AOS	Aft Optical Subsystem
ACS	Attitude Control System
AP	Archive Package
CAP	Commissioning Analysis Plan
CAR	Commissioning Activity Request
CC	MIRI Cryo-Cooler
DHAS	Data Handling and Analysis System
DOF	Degree of Freedom
EE	Encircled Energy PSF metric
GS	Guide star
FSM	Fine Steering Mirror
FP	Fine Phasing
HGA	High Gain Antenna
ISIM	Integrated SI Module
JT	Joule-Thompson stage of the MIRI CC
LOS	Line-of-Sight
MCS	Mirror Control Software
MIMF	Multi Instrument Multi Field
MIRI	Mid-InfraRed Instrument for JWST
MSE	Mission Systems Engineering
NGAS	Northrup-Grumman Aerospace Systems
OPD	Optical Path Difference
OSS	Operations Scripts Subsystem
OTE	Optical Telescope Element
OTIS	OTE-ISIM
PM	Primary Mirror
PMBA	Primary Mirror Backplane Assembly
PRMS	Phase Retrieval Metrology System
PS	Project Science Team
PSD	Power Spectral Density
PSF	Point Spread Function
PT	Pulse Tube stage of the MIRI CC
RWA	Reaction Wheel Assembly
SCA	Sensor Chip Assembly
SI	Science Instrument
SM	Secondary Mirror
STScI	Space Telescope Science Institute
SUR	Segment Update Request
TA	Target Acquisition
TBD	To Be Determined
TBR	To Be Resolved
WAS	Wavefront Analysis Software
WEx	WFS&C Executive
WFE	Wavefront Error

WFS Wavefront Sensing

11.0 APPENDIX A: LIST OF LOS MEASUREMENT NOTIFIED PARTIES

The following list was used to inform interested parties of the results of the LOS jitter measurements during early portion of JWST commissioning, in particular during the CC state transitions. Parties denoted by an asterisk, primarily dynamics engineers interested in trending the behavior (especially as the RWA speeds varied), and the WFS&C team leads, continued to receive notifications through the WF maintenance phase of commissioning and into the Cy-1 program.

Luis Meza	luis.meza@ngc.com	SE	
Keith Parrish	keith.a.parrish@nasa.gov	SE	
Julie Van Campen	julie.m.vancampen@nasa.gov	SE	*
Greg Andersen	greg.andersen@nasa.gov	SE	
Greg Walsh	gregory.j.walsh@nasa.gov	SE	*
Gary Mosier	gary.e.mosier@nasa.gov	SE	*
Carl Blaurock	carl.blaurock@nasa.gov	SE	*
Sandra Irish	sandra.m.irish@nasa.gov	SE	*
Marie Levine-West	marie.b.levine-west@jpl.nasa.gov	SE	*
Margaret Jordan	mjordan@stsci.edu	SE	
Mike Menzel	michael.t.menzel@nasa.gov	SE	
Erin Wolf	erin.wolf@ballaerospace.com	SE	
Paul Lightsey	paul.lightsey@ballaerospace.com	SE	
Scott Knight	john.knight@ballaerospace.com	SE	
Peiman Maghami	peiman.g.maghami@nasa.gov	LOS	*
Begoña Vila	maria.b.vilacostas@nasa.gov	LOS	
Chunlei Rui	Chunlei.Rui@ngc.com	ACS	
Chris Tsukamoto	chris.tsukamoto@ngc.com	ACS	
Henry Fu	Henry.Fu@ngc.com	ACS	
Kim Banks	kimberly.a.banks@nasa.gov	CC	
Bret Naylor	bret.j.naylor@jpl.nasa.gov	CC	
Mark Weilert	mark.a.weilert@jpl.nasa.gov	CC	
Analyn Schneider	analyn.c.schneider@jpl.nasa.gov	CC	
Randy Kimble	randy.a.kimble@nasa.gov	SCI	
Chuck Bowers	charles.w.bowers@nasa.gov	SCI	
Susan Neff	Susan.G.Neff@nasa.gov	SCI	
Chris Stark	christopher.c.stark@nasa.gov	SCI	
Scott Friedman	friedman@stsci.edu	SCI	
Mike McElwain	michael.w.mcelwain@nasa.gov	SCI	
Jane Rigby	jane.r.rigby@nasa.gov	SCI	
Erin Smith	erin.c.smith@nasa.gov	SCI	
George Hartig	ghartig@stsci.edu	WF	*
Lee Feinberg	lee.d.feinberg@nasa.gov	WF	*
Ritva Keski-Kuha	ritva.a.keski-kuha@nasa.gov	WF	*

Marshall Perrin	mperrin@stsci.edu	WF	*
Matt Lallo	lallo@stsci.edu	WF	*
Charles Lajoie	lajoie@stsci.edu	WF	*
Tom Comeau	tcomeau@stsci.edu	WF	*
Mike Regan	mregan@stsci.edu	WF	*
Tracy Beck	tbeck@stsci.edu	WF	*
Laura Coyle	laura.coyle@ballaerospace.com	WF	
Derek Sabatke	derek.sabatke@ballaerospace.com	WF	
Tom Zielinski	thomas.p.zielinski@nasa.gov	WF	
Carl Reis	carl.a.reis@nasa.gov	MOM	
Neil Rowlands	neil.rowlands@honeywell.com	FGS	
Gerry Warner	gerald.warner@honeywell.com	FGS	
Chris Moller	christopher.d.moller@nasa.gov	FGS	
Julia Zhou	julia.zhou2@honeywell.com	FGS	
Scott Lambros	scott.d.lambros@nasa.gov	SI	
Amy Delisa	amy.s.delisa@nasa.gov	SI	

12.0 APPENDIX B: LOG OF LOS JITTER MEASUREMENTS

obs date	MJD	filename	FOF name	ana	Xrms	Yrms	Jmas	RJmas	RWA1	RWA2	RWA3	RWA4	RWA5	RWA6	JTfreq	PTfreq	JTdrv	PTdrv
3/17/2022 8:05	59655.33732	jw01163002001_03102_00001_nrca3	FOFWSS2022076143955038	g: 60/900	0.023	0.025	1.04	0.65	24.5798	40.4919	45.4876	24.6779	45.5047	31.485	88.028	30.488	0	49.998
3/21/2022 5:26	59659.22668	jw01161001001_03102_00001_nrca3	CCJ_FOF_cat_1	g: 60/900	0.026	0.026	1.13	0.76	41.7554	26.9912	43.0937	27.0758	33.0927	43.0615	88.028	30.488	0	49.999
3/21/2022 5:30	59659.22983	jw01161001001_03102_00002_nrca3	CCJ_FOF_cat_1	g: 60/900	0.024	0.026	1.1	0.71	41.7711	26.9903	43.095	27.0724	33.0719	43.0628	88.028	30.488	0	49.999
3/21/2022 5:35	59659.23298	jw01161001001_03102_00003_nrca3	CCJ_FOF_cat_1	g: 60/900	0.026	0.026	1.13	0.76	41.7921	26.9845	43.095	27.069	33.047	43.0669	88.028	30.488	0	49.999
3/21/2022 5:40	59659.23614	jw01161001001_03102_00004_nrca3	CCJ_FOF_cat_1	g: 60/900	0.027	0.026	1.16	0.8	41.8032	26.9836	43.1045	27.069	33.0304	43.0669	88.028	30.488	0	49.999
3/21/2022 5:44	59659.2393	jw01161001001_03102_00005_nrca3	CCJ_FOF_cat_1	g: 60/900	0.025	0.026	1.13	0.76	41.8235	26.9778	43.1045	27.0622	33.0055	43.0735	88.028	30.488	0	49.999
3/23/2022 4:57	59661.20653	jw01161013001_03102_00001_nrca3	CCJFOFWSS2022082053118292	g: 60/900	0.03	0.036	1.45	1.15	47.2805	22.7381	47.3456	32.552	22.8007	41.8398	88.028	30.488	8.6	64.955
3/23/2022 5:01	59661.20968	jw01161013001_03102_00002_nrca3	CCJFOFWSS2022082053118292	g: 60/900	0.03	0.037	1.48	1.19	47.2892	22.7268	47.3574	32.5725	22.795	41.8451	88.028	30.488	8.6	64.955
3/23/2022 5:06	59661.21283	jw01161013001_03102_00003_nrca3	CCJFOFWSS2022082053118292	g: 60/900	0.032	0.036	1.49	1.2	47.301	22.7202	47.3632	32.5928	22.7893	41.8451	88.028	30.488	8.6	64.955
3/23/2022 5:11	59661.216	jw01161013001_03102_00004_nrca3	CCJFOFWSS2022082053118292	g: 60/900	0.031	0.036	1.48	1.19	47.3041	22.7098	47.3751	32.6167	22.7779	41.8398	88.028	30.488	8.6	64.955
3/23/2022 5:15	59661.21915	jw01161013001_03102_00005_nrca3	CCJFOFWSS2022082053118292	g: 60/900	0.032	0.037	1.53	1.25	47.3159	22.7042	47.3811	32.6337	22.7694	41.8451	88.028	30.488	8.6	64.955
3/23/2022 8:23	59661.34998	jw01163008001_03102_00001_nrca3	CCJFOFTLM2022082185219506	g: 60/900	0.032	0.042	1.63	1.37	47.6452	22.376	47.7109	33.479	22.4385	41.8346	88.028	30.488	8.6	64.971
3/24/2022 22:59	59662.95807	jw01163009001_03102_00001_nrca3	CCJFOFTLM2022083231108672	g: 60/900	0.049	0.066	2.55	2.31	51.3016	18.7141	51.3722	43.4028	18.7816	42.8468	88.028	30.488	8.6	64.961
3/27/2022 14:41	59665.61194	jw01163012001_03102_00001_nrca3	CCJFOFTLM2022086175946997	g: 60/900	0.026	0.033	1.3	1.02	35.0366	49.5428	37.1651	20.5736	49.6094	20.5065	88.028	30.488	8.6	65.003
3/28/2022 14:16	59666.59474	jw01163013001_03102_00001_nrca3	CCJFOFTLM2022087185750441	g: 60/900	0.025	0.029	1.18	0.87	36.4128	48.5208	39.833	21.5966	48.5755	21.5313	88.028	30.488	8.6	65.003
3/29/2022 14:37	59667.60953	jw01163014001_03102_00001_nrca3	CCJFOFTLM2022088184119904	g: 60/900	0.029	0.031	1.32	1.05	37.8551	47.699	42.0657	22.4214	47.7589	22.3534	88.028	30.488	8.6	64.929
3/31/2022 13:57	59669.58175	jw01163015001_03102_00001_nrca3	CCJFOFTLM2022090165541056	g: 60/900	0.029	0.035	1.41	1.15	32.4831	43.3973	45.1524	25.018	45.1684	24.9497	88.028	30.488	8.6	65.003
4/1/2022 14:07	59670.5882	jw01163016001_03102_00001_nrca3	CCJFOFTLM2022091141526688	g: 60/900	0.028	0.033	1.33	1.05	34.317	41.877	43.9453	26.2295	43.9563	26.1725	88.028	30.488	8.6	65.003
4/2/2022 16:45	59671.69807	jw01163017001_03102_00001_nrca3	CCJFOFTLM2022092181550188	g: 60/900	0.024	0.025	1.07	0.72	31.1112	38.968	44.3063	25.853	44.3249	25.7902	88.028	30.488	8.6	64.961
4/3/2022 13:49	59672.57622	jw01163018001_03102_00001_nrca3	CCJFOFTLM2022093184414406	g: 60/900	0.023	0.028	1.13	0.77	43.7935	26.2253	43.8594	41.2072	36.6808	26.2418	88.028	30.488	8.6	64.985
4/4/2022 15:36	59673.65013	jw01163019001_03102_00001_nrca3	CCJFOFTLM2022094184501948	g: 60/900	0.023	0.025	1.04	0.68	24.752	34.5902	45.3154	24.8494	45.3324	24.89	88.028	30.488	8.6	65.003
4/5/2022 15:07	59674.62993	jw01163020001_03102_00001_nrca3	CCJFOFTLM2022095171409229	g: 60/900	0.026	0.026	1.13	0.8	24.3457	30.4695	45.7242	24.4425	45.733	28.6745	88.028	30.488	8.6	65.003
4/6/2022 12:08	59675.50609	jw01410130001_03102_00001_nrca3	CCJFOFTLM2022096130724211	g: 60/900	0.024	0.025	1.09	0.75	24.3349	29.6187	45.7272	24.4332	45.7445	27.7489	88.028	30.488	8.6	63.204
4/6/2022 12:30	59675.52096	jw01410131001_03102_00001_nrca3	CCJFOFTLM2022096131627678	g: 60/900	0.024	0.026	1.09	0.75	24.3657	29.5149	45.7043	24.4607	45.7215	27.7904	88.028	30.488	8.6	63.102
4/6/2022 12:48	59675.5337	jw01410132001_03102_00001_nrca3	CCJFOFTLM2022096131937807	g: 60/900	0.025	0.028	1.16	0.85	24.3873	29.4275	45.6785	24.488	45.6929	27.8286	88.028	30.488	8.6	63.162
4/6/2022 13:18	59675.5542	jw01410133001_03102_00001_nrca3	CCJFOFTLM2022096134459712	g: 60/900	0.022	0.024	1	0.69	24.4242	29.4338	45.6414	24.5246	45.6528	27.8078	88.028	30.488	8.6	63.127
4/6/2022 13:40	59675.56959	jw01410134001_03102_00001_nrca3	CCJFOFTLM2022096134818972	g: 60/900	0.026	0.023	1.07	0.79	24.4493	29.3203	45.6128	24.5491	45.63	27.8538	88.028	30.488	8.6	62.966
4/6/2022 14:10	59675.59032	jw01410136001_03102_00001_nrca3	CCJFOFTLM2022096165314386	g: 60/900	0.022	0.026	1.05	0.76	24.4825	29.1669	45.5843	24.58	45.5957	27.9135	88.028	30.488	8.6	62.771
4/6/2022 14:34	59675.60744	jw01410137001_03102_00001_nrca3	CCJFOFTLM2022096144622193	g: 60/900	0.025	0.022	1.03	0.73	24.5094	29.044	45.5615	24.6043	45.5729	27.9668	88.028	30.488	8.6	62.879
4/6/2022 15:23	59675.64142	jw01163021001_03102_00001_nrca3	CCJFOFTLM2022096223905505	g: 60/900	0.024	0.026	1.09	0.74	24.5645	28.6975	45.5012	24.6625	45.5184	28.1602	88.028	30.488	8.6	63.096
4/7/2022 14:11	59676.59139	jw01163022001_03102_00001_nrca3	CCJFOFTLM2022097164426837	g: 60/900	0.024	0.024	1.05	0.7	31.2004	25.3023	44.7871	25.3883	44.7927	34.8525	88.028	30.488	45	57.826
4/8/2022 18:04	59677.75309	jw01163023001_03102_00001_nrca3	CCJFOFTLM2022098194727140	g: 60/900	0.024	0.025	1.06	0.72	43.354	25.0714	45.0167	25.1563	43.1379	44.9779	88.028	30.488	45	49.29
4/9/2022 13:32	59678.56399	jw01163024001_03102_00001_nrca3	CCJFOFTLM2022099153939771	g: 60/900	0.022	0.024	1	0.64	46.1375	23.8824	46.2066	23.9646	36.2094	44.067	88.028	30.488	45	50.747
4/11/2022 13:52	59680.578	jw01163025001_03102_00001_nrca3	CCJFOFTLM2022101162553001	g: 60/900	0.025	0.025	1.1	0.74	47.8277	33.9305	22.2411	27.7316	47.9136	22.2048	88.028	30.488	45	51.06
4/12/2022 4:02	59681.16867	jw01170001001_03102_00001_nrca3	CCJFOFTLM2022102112353115	g: 60/900	0.023	0.026	1.08	0.71	46.6948	29.4165	23.375	27.7282	46.7717	23.3449	88.028	30.488	45	50.785
4/12/2022 4:07	59681.17183	jw01170001001_03102_00002_nrca3	CCJFOFTLM2022102112353115	g: 60/900	0.188	0.077	6.29	6.24	46.6837	29.3934	23.3809	27.7386	46.7658	23.3454	88.028	30.488	45	50.785
4/12/2022 4:11	59681.175	jw01170001001_03102_00003_nrca3	CCJFOFTLM2022102112353115	g: 60/900	0.024	0.025	1.07	0.69	46.6831	29.3655	23.3918	27.7213	46.7599	23.3543	88.028	30.488	45	50.785
4/12/2022 4:16	59681.17816	jw01170001001_03102_00004_nrca3	CCJFOFTLM2022102112353115	g: 60/900	0.025	0.025	1.09	0.73	46.672	29.3388	23.3948	27.7213	46.754	23.3602	88.028	30.488	45	50.785
4/12/2022 4:21	59681.18132	jw01170001001_03102_00005_nrca3	CCJFOFTLM2022102112353115	g: 60/900	0.025	0.026	1.1	0.74	46.6656	29.3152	23.4004	27.7211	46.7482	23.3661	88.028	30.488	45	50.785
4/12/2022 17:40	59681.73673	jw01163026001_03102_00001_nrca3	CCJFOFTLM2022102194045617	g: 60/900	0.025	0.025	1.09	0.73	46.6136	25.4832	23.4551	28.3692	46.6896	23.4229	88.028	30.488	45	49.114
4/13/2022 20:04	59682.8365	jw01163027001_03102_00001_nrca3	CCJFOFTLM2022103231020135	g: 60/900	0.024	0.025	1.08	0.71	47.3041	22.7098	24.2484	33.7081	47.3871	22.7268	88.028	30.488	45	52.029
4/13/2022 22:13	59682.92622	jw01439001001_03102_00001_nrca3	CCJFOFTLM2022104003327152	g: 60/1800	0.023	0.026	1.09	0.72	47.3544	22.6646	25.1091	34.7373	47.4345	22.6787	88.028	30.488	45	51.859
4/13/2022 22:18	59682.92939	jw01439001001_03102_00002_nrca3	CCJFOFTLM2022104003327152	g: 60/1800	0.025	0.026	1.1	0.74	47.3544	22.6646	25.1437	34.7722	47.4345	22.6787	88.028	30.488	45	51.85
4/13/2022 22:22	59682.93252	jw01439001001_03102_00003_nrca3	CCJFOFTLM2022104003327152	g: 60/1800	0.025	0.026	1.11	0.75	47.3544	22.6618	25.169	34.809	47.4345	22.6759	88.028	30.488	45	51.861
4/13/2022 22:27	59682.93568	jw01439001001_03102_00004_nrca3	CCJFOFTLM2022104003327152	g: 60/1800	0.024	0.026	1.1	0.74	47.3573	22.659	25.2069	34.8453	47.443	22.6759	88.028	30.488	60	51.861

obs date	MJD	filename	FOF name	ana	Xrms	Yrms	Jmas	RJmas	RWA1	RWA2	RWA3	RWA4	RWA5	RWA6	JTfreq	PTfreq	JTdrv	PTdrv
4/13/2022 22:31	59682.93883	jw01439001001_03102_00005_nrca3	CCJFOFTLM2022104003327152	g: 60/1800	0.025	0.026	1.12	0.77	47.3604	22.659	25.234	34.8875	47.4464	22.6731	88.028	30.488	60	51.861
4/13/2022 22:36	59682.942	jw01439001001_03102_00006_nrca3	CCJFOFTLM2022104003327152	g: 60/1800	0.025	0.027	1.13	0.78	47.3632	22.6534	25.2673	34.9181	47.443	22.6731	88.028	30.488	60	51.861
4/13/2022 22:41	59682.94516	jw01439001001_03102_00007_nrca3	CCJFOFTLM2022104003327152	g: 60/1800	0.024	0.025	1.08	0.71	47.3632	22.6534	25.2992	34.9662	47.4464	22.6703	88.028	30.488	60	51.861
4/13/2022 22:45	59682.94831	jw01439001001_03102_00008_nrca3	CCJFOFTLM2022104003327152	g: 60/1800	0.026	0.026	1.14	0.8	47.3632	22.6534	25.3357	34.9978	47.4464	22.6703	88.028	30.488	45	52.1
4/13/2022 22:50	59682.95148	jw01439001001_03102_00009_nrca3	CCJFOFTLM2022104003327152	g: 60/1800	0.025	0.026	1.11	0.75	47.3662	22.6506	25.3649	35.0366	47.4496	22.6675	88.028	30.488	45	53.355
4/13/2022 22:54	59682.95463	jw01439001001_03102_00010_nrca3	CCJFOFTLM2022104003327152	g: 60/1800	0.025	0.026	1.13	0.78	47.3692	22.6506	25.404	35.0719	47.4464	22.6675	88.028	30.488	45	53.947
4/13/2022 22:59	59682.9578	jw01439001001_03102_00011_nrca3	CCJFOFTLM2022104003327152	g: 60/1800	0.024	0.026	1.1	0.74	47.3723	22.6477	25.432	35.1119	47.4549	22.6646	88.028	30.488	45	54.287
4/13/2022 23:03	59682.96096	jw01439001001_03102_00012_nrca3	CCJFOFTLM2022104003327152	g: 60/1800	0.025	0.027	1.13	0.78	47.3723	22.6449	25.4613	35.1472	47.4549	22.659	88.028	30.488	45	54.43
4/13/2022 23:08	59682.96409	jw01439001001_03102_00013_nrca3	CCJFOFTLM2022104003327152	g: 60/1800	0.025	0.026	1.12	0.77	47.3751	22.6449	25.5022	35.1913	47.4549	22.6618	88.028	30.488	45	54.466
4/13/2022 23:12	59682.96725	jw01439001001_03102_00014_nrca3	CCJFOFTLM2022104003327152	g: 60/1800	0.023	0.026	1.08	0.71	47.3751	22.6421	25.5281	35.222	47.4583	22.659	88.028	30.488	45	54.467
4/13/2022 23:17	59682.97038	jw01439001001_03102_00015_nrca3	CCJFOFTLM2022104003327152	g: 60/1800	0.025	0.025	1.11	0.75	47.3751	22.6393	25.56	35.2619	47.4583	22.659	88.028	30.488	45	54.437
4/13/2022 23:21	59682.97354	jw01439001001_03102_00016_nrca3	CCJFOFTLM2022104003327152	g: 60/1800	0.026	0.027	1.15	0.81	47.378	22.6365	25.5978	35.2971	47.4642	22.6534	88.028	30.488	45	54.348
4/13/2022 23:26	59682.9767	jw01439001001_03102_00017_nrca3	CCJFOFTLM2022104003327152	g: 60/1800	0.024	0.026	1.11	0.75	47.381	22.6337	25.6233	35.336	47.4642	22.6534	88.028	30.488	45	54.253
4/13/2022 23:30	59682.97985	jw01439001001_03102_00018_nrca3	CCJFOFTLM2022104003327152	g: 60/1800	0.024	0.026	1.09	0.72	47.381	22.6337	25.6585	35.3757	47.4641	22.6506	88.028	30.488	45	54.125
4/13/2022 23:35	59682.98302	jw01439001001_03102_00019_nrca3	CCJFOFTLM2022104003327152	g: 60/1800	0.024	0.026	1.09	0.72	47.3869	22.6337	25.6841	35.4066	47.4641	22.6477	88.028	30.488	45	53.997
4/13/2022 23:40	59682.98617	jw01439001001_03102_00020_nrca3	CCJFOFTLM2022104003327152	g: 60/1800	0.025	0.028	1.15	0.81	47.3869	22.6309	25.7194	35.4508	47.4667	22.6491	88.028	30.488	45	53.896
4/13/2022 23:44	59682.98932	jw01439001001_03102_00021_nrca3	CCJFOFTLM2022104003327152	g: 60/1800	0.024	0.026	1.1	0.74	47.3869	22.6281	25.7484	35.4862	47.4702	22.6477	88.028	30.488	45	53.741
4/13/2022 23:49	59682.99249	jw01439001001_03102_00022_nrca3	CCJFOFTLM2022104003327152	g: 60/1800	0.023	0.026	1.08	0.71	47.3869	22.6281	25.7821	35.5218	47.4702	22.6477	88.028	30.488	45	53.622
4/13/2022 23:53	59682.99564	jw01439001001_03102_00023_nrca3	CCJFOFTLM2022104003327152	g: 60/1800	0.025	0.029	1.17	0.84	47.3898	22.6253	25.813	35.5688	47.4702	22.6449	88.028	30.488	45	53.518
4/13/2022 23:58	59682.9988	jw01439001001_03102_00024_nrca3	CCJFOFTLM2022104003327152	g: 60/1800	0.025	0.026	1.1	0.74	47.3929	22.6225	25.8422	35.5999	47.4702	22.6393	88.028	30.488	45	53.429
4/14/2022 0:02	59683.00197	jw01439001001_03102_00025_nrca3	CCJFOFTLM2022104003327152	g: 60/1800	0.025	0.025	1.1	0.74	47.396	22.6225	25.8787	35.6355	47.4786	22.6393	88.028	30.488	45	53.32
4/14/2022 0:07	59683.00512	jw01439001001_03102_00026_nrca3	CCJFOFTLM2022104003327152	g: 60/1800	0.025	0.027	1.13	0.78	47.3988	22.6209	25.9138	35.6756	47.4786	22.6393	88.028	30.488	45	53.239
4/14/2022 0:11	59683.00829	jw01439001001_03102_00027_nrca3	CCJFOFTLM2022104003327152	g: 60/1800	0.024	0.026	1.1	0.74	47.3988	22.6181	25.9436	35.7114	47.4786	22.6365	88.028	30.488	45	53.147
4/14/2022 12:29	59683.52024	jw01163028001_03102_00001_nrca3	CCJFOFTLM2022104141247011	g: 60/900	0.029	0.027	1.22	0.91	47.7049	22.3111	30.7424	41.6199	47.7843	22.3252	88.028	30.488	45	51.963
4/15/2022 10:29	59684.43692	jw01163029001_03102_00001_nrca3	CCJFOFTLM2022105133958691	g: 60/900	0.024	0.029	1.18	0.85	48.708	21.3161	37.2909	48.8037	46.0226	21.3322	88.028	30.488	45	51.957
4/15/2022 23:46	59684.99083	jw01163030001_03102_00001_nrca3	CCJFOFTLM2022106004314882	g: 60/900	0.023	0.026	1.08	0.71	49.7538	20.2639	39.1469	49.8498	42.5125	20.2791	88.028	30.488	45	52.139
4/21/2022 15:22	59690.64035	jw01163031001_03102_00001_nrca3	CCJFOFTLM2022112093949215	g: 60/900	0.022	0.025	1.03	0.63	22.105	22.0885	7.96093	22.2048	1.75927	22.0666	88.028	30.488	45	52.247
4/23/2022 4:45	59692.1982	jw01467001001_03102_00001_nrca3	CCJFOFTLM2022113131618242	g: 60/900	0.023	0.024	1.03	0.62	25.3215	25.3055	11.1563	25.4206	12.5902	25.288	88.028	30.488	45	52.2
4/26/2022 3:10	59695.13209	jw01163033001_03102_00001_nrca3	CCJFOFTLM2022116110255056	g: 60/900	0.024	0.025	1.08	0.7	35.7025	34.3165	35.7671	35.231	34.3849	34.7854	88.028	30.488	45	52.213
4/28/2022 12:00	59697.50067	jw01163050001_03102_00001_nrca3	CCJFOFTLM2022118123538894	g: 60/900	0.025	0.026	1.13	0.78	40.2188	29.7927	40.2924	39.1921	29.86	36.9004	88.028	30.488	45	52.927
4/30/2022 16:47	59699.69995	jw01163051001_03102_00001_nrca3	CCJFOFTLM2022120174221863	g: 60/900	0.026	0.025	1.12	0.77	43.9893	26.0254	44.0586	42.4963	26.0906	37.7156	88.028	30.488	45	51.823
5/2/2022 15:43	59701.65533	jw01163052001_03102_00001_nrca3	CCJFOFTLM2022122162059487	g: 60/900	0.028	0.025	1.17	0.84	47.31	22.7098	47.3751	45.59	22.7779	37.8598	88.028	30.488	45	52.204
5/5/2022 16:22	59704.68262	jw01163053001_03102_00001_nrca3	CCJFOFTLM2022125180854960	g: 60/900	0.023	0.025	1.04	0.63	36.9548	33.0636	36.9734	37.0572	33.1302	35.3889	88.028	30.488	45	53.465
5/7/2022 21:53	59706.91191	jw01163054001_03102_00001_nrca3	CCJFOFTLM2022127234627142	g: 60/900	0.023	0.025	1.06	0.68	40.4767	29.5412	38.5251	40.5831	29.6076	35.019	88.028	30.488	45	52.206
5/20/2022 9:13	59719.38444	jw01163055001_03102_00001_nrca3	CCJFOFTLM2022140111510181	g: 60/900	0.022	0.025	1.05	0.66	19.4636	19.4489	19.5288	3.23868	19.3777	5.86861	88.028	30.488	45	52.215
5/21/2022 1:32	59720.06448	jw01163056001_03102_00001_nrca3	CCJFOFTLM2022141105422340	g: 60/900	0.023	0.026	1.07	0.7	21.4477	21.4294	21.5113	5.60751	21.3564	5.88809	88.028	30.488	45	52.401
5/22/2022 17:21	59721.72316	jw01163057001_03102_00001_nrca3	CCJFOFTLM2022143004139717	g: 60/900	0.021	0.024	1	0.6	23.5394	23.5219	23.609	3.90166	23.4668	7.2917	88.028	30.488	45	52.143
5/24/2022 19:17	59723.80391	jw01163058001_03102_00001_nrca3	CCJFOFTLM2022145111727986	g: 60/900	0.024	0.03	1.18	0.79	6.73872	26.7932	5.00099	26.676	26.859	26.7429	88.028	30.488	45	51.322
5/27/2022 0:14	59726.01041	jw01163059001_03102_00001_nrca3	CCJFOFTLM2022147115334246	g: 60/900	0.023	0.025	1.06	0.61	35.7314	34.432	34.3335	35.8342	34.3549	34.3977	88.028	30.488	45	52.016
6/1/2022 16:56	59731.70602	jw01163062001_03102_00001_nrca3	CCJFOFTLM2022152175926259	g: 60/900	0.027	0.028	1.2	0.8	41.724	28.2919	41.3877	41.8288	39.6898	28.3062	88.028	30.488	45	52.323
6/3/2022 19:32	59733.81393	jw01163167001_03102_00001_nrca3	CCJFOFTLM2022155024120283	g: 60/900	0.026	0.027	1.17	0.8	36.978	40.8785	43.6362	26.5269	43.6525	26.467	88.028	30.488	45	52.23
6/5/2022 21:49	59735.90957	jw01163168001_03102_00001_nrca3	CCJFOFTLM2022157002639347	g: 60/900	0.025	0.028	1.16	0.78	36.3357	38.0277	43.6951	26.471	43.7072	26.4088	88.028	30.488	45	52.523
6/8/2022 1:18	59738.0546	jw01163169001_03102_00001_nrca3	CCJFOFTLM2022159110854599	g: 60/900	0.027	0.03	1.24	0.88	36.8945	35.0366	43.3756	26.7951	43.3866	26.7286	88.028	30.488	45	49.967
6/10/2022 10:04	59740.42004	jw01163170001_03102_00001_nrca3	CCJFOFTLM2022161112855633	g: 72/750	0.028	0.032	1.32	0.75	35.3633	32.279	43.2079	26.9531	43.2294	26.8905	88.028	30.488	45	52.247
6/12/2022 6:39	59742.27748	jw01163171001_03102_00001_nrca3	CCJFOFTLM2022163105903705	g: 72/750	0.032	0.031	1.38	0.89	43.5708	26.4481	42.3707	42.5922	43.6525	26.4637	88.028	30.488	45	52.143
6/14/2022 11:50	59744.49325	jw01163172001_03102_00001_nrca3	CCJFOFTLM2022165141933088	g: 72/750	0.033	0.034	1.46	0.93	44.6466	25.3748	44.7137	25.4584	27.298	25.5246	88.028	30.488	45	52.053
6/16/2022 4:31	59746.18837	jw01163173001_03102_00001_nrca3	CCJFOFTLM2022169120809852	g: 72/750	0.033	0.036	1.49	0.92	45.321	24.6964	45.3875	24.7783	32.1602	32.3771	88.028	30.488	45	52.435
6/18/2022 2:17	59748.09536	jw01163174001_03102_00001_nrca3	CCJFOFTLM2022169121947883	g: 72/750	0.03	0.033	1.38	0.83	32.6291	24.4886	45.5933	24.5737	45.6071	26.8905	88.028	30.488	45	52.63

obs date	MJD	filename	FOF name	ana	Xrms	Yrms	Jmas	RJmas	RWA1	RWA2	RWA3	RWA4	RWA5	RWA6	JTfreq	PTfreq	JTdrv	PTdrv
6/19/2022 16:32	59749.68953	jw01163200001_03102_00001_nrca3	CCJFOFTLM2022170200539373	g: 60/900	0.02	0.027	1.04	0.75	45.6014	37.8124	40.4868	24.4977	45.6814	24.4354	88.028	30.488	45.000	52.407
6/20/2022 2:12	59750.0923	jw01163202001_03102_00001_nrca3	CCJFOFTLM2022171111335302	g: 60/900	0.021	0.024	0.99	0.68	45.0055	33.6397	39.0787	25.0933	45.0896	25.0213	88.028	30.488	45.000	52.276
6/21/2022 13:55	59751.58014	jw01163175001_03102_00001_nrca3	CCJFOFTLM2022172173036092	g: 72/750	0.03	0.034	1.4	0.77	45.5558	24.4577	45.6243	24.543	35.7537	31.1848	88.028	30.488	45.000	52.415
6/27/2022 13:25	59757.55939	jw01163206001_04102_00001_nrca3	CCJFOFTLM2022178134859017	g: 72/750	0.034	0.032	1.45	0.98	48.6913	21.3214	48.7611	46.4563	38.9757	21.3376	88.028	30.488	45.000	52.595
6/29/2022 14:58	59759.62386	jw02726477001_03102_00001_nrca3	CCJFOFTLM2022180221634422	g: 72/750	0.029	0.033	1.36	0.83	49.597	20.4197	21.2786	31.4889	49.6779	20.4352	88.028	30.488	45.000	52.618
7/1/2022 13:04	59761.54483	jw02724067001_03102_00001_nrca3	CCJFOFTLM2022182132338928	g: 72/750	0.031	0.032	1.39	0.83	50.9539	19.0661	40.0691	51.0557	43.3159	19.0817	88.028	30.488	45.000	52.428
7/4/2022 16:11	59764.67476	jw02586022001_03102_00001_nrca3	CCJFOFTLM2022185222052966	g: 72/750	0.029	0.032	1.35	0.82	50.9476	19.0667	31.5874	31.4615	51.043	19.083	88.028	30.488	45.000	52.456
7/6/2022 11:48	59766.49213	jw02725097001_03102_00001_nrca3	CCJFOFTLM2022187121315239	g: 72/750	0.032	0.034	1.44	0.94	50.9095	19.1074	50.9788	19.1913	37.2811	26.1555	88.028	30.488	45.000	52.723
7/8/2022 16:15	59768.67753	jw02726227001_03102_00001_nrca3	CCJFOFTLM2022190001725220	g: 72/750	0.031	0.033	1.4	0.88	51.7167	33.3494	36.2277	18.3901	51.804	18.3185	88.028	30.488	45.000	52.410
7/10/2022 11:30	59770.47976	jw02725187001_03102_00001_nrca3	CCJFOFTLM2022191163320797	g: 72/750	0.036	0.04	1.66	1.20	51.1799	18.8355	51.2465	18.9199	46.7717	28.0439	88.028	30.488	45.000	52.447
7/12/2022 15:50	59772.65993	jw02726027001_03102_00001_nrca3	CCJFOFTLM2022194110852390	g: 72/750	0.037	0.037	1.62	1.09	41.1611	34.7569	54.1518	16.0091	54.1724	15.9445	88.028	30.488	45.000	52.241
7/15/2022 9:58	59775.41557	jw02726162001_03102_00001_nrca3	CCJFOFTLM2022196112541893	g: 72/750	0.038	0.038	1.67	1.15	51.5354	32.4952	43.6689	18.5646	51.6129	18.4974	88.028	30.488	45.000	52.659
7/17/2022 10:32	59777.43925	jw02586137001_03102_00001_nrca3	CCJFOFTLM2022198123615153	g: 72/750	0.034	0.037	1.55	1.06	52.8485	29.4531	35.8476	17.2526	52.9342	17.1823	88.028	30.488	45.000	52.628
7/19/2022 15:33	59779.64799	jw02724232001_03102_00001_nrca3	CCJFOFTLM2022200175517786	g: 72/750	0.031	0.032	1.38	0.84	54.5657	15.4521	54.6283	44.7362	39.0265	15.4657	88.028	30.488	45.000	52.314
7/22/2022 8:53	59782.37076	jw02725417001_03102_00001_nrca3	CCJFOFTLM2022203114643719	g: 72/750	0.034	0.036	1.54	1.05	53.0201	22.2774	48.0684	17.0812	53.0997	17.0144	88.028	30.488	45.000	52.592
7/24/2022 15:08	59784.63103	jw02726492001_03102_00001_nrca3	CCJFOFTLM2022205155345132	g: 72/750	0.035	0.038	1.61	1.08	51.6778	21.0488	18.3898	41.6771	51.7652	18.3577	88.028	30.488	45.000	52.372
7/26/2022 16:51	59786.70271	jw02725387001_03102_00001_nrca3	CCJFOFTLM2022207174711602	g: 72/750	0.031	0.033	1.4	0.85	31.1268	17.5421	52.5336	17.626	52.5534	17.6456	88.028	30.488	45.000	52.410
7/28/2022 19:01	59788.79302	jw02726037001_03102_00001_nrca3	CCJFOFTLM2022209193538017	g: 72/750	0.035	0.037	1.57	1.02	52.4744	17.538	38.7855	18.9775	52.5534	17.5554	88.028	30.488	45.000	52.525
7/30/2022 14:11	59790.59128	jw02586024001_03102_00001_nrca3	CCJFOFTLM2022211221058382	g: 72/750	0.031	0.033	1.41	0.92	53.113	16.9038	17.8568	23.3278	53.1961	16.9186	88.028	30.488	45.000	52.433
8/1/2022 15:24	59792.64216	jw02586057001_03102_00001_nrca3	CCJFOFTLM2022214104107611	g: 72/750	0.034	0.037	1.55	0.98	53.1463	18.5547	16.9186	20.8229	53.2294	16.8828	88.028	30.488	45.000	52.654
8/5/2022 12:51	59796.53556	jw02586023001_03102_00001_nrca3	CCJFOFTLM2022221130328130	g: 72/750	0.03	0.033	1.39	0.87	51.3401	18.6771	31.0682	28.2954	51.4194	18.6956	88.028	30.488	45.000	52.502
8/10/2022 4:01	59801.16805	jw02725389001_04102_00001_nrca3	CCJFOFTLM2022222212312292	g: 72/750	0.031	0.038	1.52	1.04	53.8078	16.2072	53.8737	25.1942	31.5993	16.2229	88.028	30.488	45.000	52.573
8/12/2022 17:53	59803.74534	jw02586237001_03102_00001_nrca3	CCJFOFTLM2022224222834438	g: 72/750	0.031	0.032	1.39	0.85	39.6647	18.4226	51.6596	18.5054	51.6778	18.6195	88.028	30.488	45.000	52.638
8/15/2022 10:36	59806.44193	jw02586202001_03102_00001_nrca3	CCJFOFTLM2022227220753992	g: 72/750	0.031	0.034	1.42	0.85	54.1586	15.8593	54.2263	15.9406	25.9412	23.0918	88.028	30.488	45.000	52.863
8/16/2022 11:33	59807.48185	jw02725388001_03102_00001_nrca3	CCJFOFTLM2022228140245361	g: 72/750	0.035	0.034	1.5	1.02	53.196	16.822	53.2627	38.5271	50.7391	16.8387	88.028	30.488	45.000	52.651
8/20/2022 14:43	59811.6135	jw02586067001_03102_00001_nrca3	CCJFOFTLM2022232190933289	g: 72/750	0.045	0.098	3.34	3.13	39.3438	30.6735	39.4127	30.754	31.6071	35.9827	88.028	30.488	42.750	55.175
8/22/2022 10:48	59813.4506	jw02725485001_03102_00001_nrca3	CCJFOFTLM2022234133438908	g: 72/750	0.032	0.034	1.45	0.98	40.1438	29.8688	40.212	36.1914	29.933	36.7563	88.028	30.488	45.000	52.523
8/24/2022 19:15	59815.80276	jw02725017001_03102_00001_nrca3	CCJFOFTLM2022236202247821	g: 72/750	0.03	0.035	1.43	0.99	42.2913	31.1768	27.7761	27.9192	42.3799	27.7419	88.028	30.488	45.000	54.125
8/26/2022 17:53	59817.74521	jw02586277001_03102_00001_nrca3	CCJFOFTLM2022238234633153	g: 72/750	0.03	0.033	1.38	0.87	41.0246	41.6511	41.4079	28.4608	41.7188	28.3974	88.028	30.488	45.000	52.815
8/28/2022 18:21	59819.76518	jw02586282001_03102_00001_nrca3	CCJFOFTLM2022240222916139	g: 72/750	0.04	0.037	1.69	1.20	40.0441	27.6485	42.4381	27.7282	42.454	40.8587	88.028	30.488	45.000	52.468
8/30/2022 12:17	59821.51245	jw02725452001_03102_00001_nrca3	CCJFOFTLM2022243112337023	g: 72/750	0.038	0.039	1.67	1.20	45.0279	24.9835	45.096	34.7612	25.0495	29.5743	88.028	30.488	45.000	52.486
9/1/2022 16:37	59823.69265	jw02726028001_03102_00001_nrca3	CCJFOFTLM2022245111117310	g: 72/750	0.034	0.035	1.52	1.01	46.7006	23.316	46.7708	39.1434	23.3809	30.1257	88.028	30.488	45.000	52.799
9/3/2022 13:32	59825.5645	jw02726029001_03102_00001_nrca3	CCJFOFTLM2022246160911606	g: 72/750	0.034	0.035	1.52	1.01	46.334	23.6801	46.4041	39.9741	23.7512	29.7592	88.028	30.488	45.000	52.543
9/5/2022 12:38	59827.52683	jw02726097001_03102_00001_nrca3	CCJFOFTLM2022248152540652	g: 72/750	0.034	0.037	1.55	0.96	47.077	33.7124	22.9893	47.171	23.0069	27.9389	88.028	30.488	45.000	52.857
9/7/2022 19:05	59829.79582	jw02586367001_03102_00001_nrca3	CCJFOFTLM2022250222015176	g: 72/750	0.034	0.036	1.53	1.02	35.658	23.2925	46.7893	23.3779	36.3448	46.7482	88.028	30.488	45.000	52.644
9/9/2022 15:56	59831.66439	jw02586402001_03102_00001_nrca3	CCJFOFTLM2022252172910924	g: 72/750	0.033	0.036	1.51	1.01	47.7949	22.2271	47.8528	28.9967	22.2887	46.8469	88.028	30.488	45.000	52.497
9/13/2022 0:13	59835.00907	jw02586382001_03102_00001_nrca3	CCJFOFTLM2022256110951717	g: 72/750	0.03	0.033	1.38	0.88	20.6603	33.9178	49.4028	20.7607	49.4215	34.2866	88.028	30.488	45.000	53.013
9/15/2022 12:49	59837.53447	jw02726232001_03102_00001_nrca3	CCJFOFTLM2022258235433359	g: 72/750	0.03	0.034	1.41	0.91	33.6619	48.5816	22.6038	21.5353	48.6486	21.4693	88.028	30.488	45.000	53.051
9/17/2022 20:10	59839.84037	jw02586312001_03102_00001_nrca3	CCJFOFTLM2022261112026838	g: 72/750	0.032	0.037	1.52	0.96	51.5612	18.4623	51.6208	19.602	18.5232	44.8207	88.028	30.488	45.000	52.798
9/19/2022 20:55	59841.87218	jw02725442001_03102_00001_nrca3	CCJFOFTLM2022263001909744	g: 72/750	0.028	0.031	1.29	0.72	49.5349	49.6405	20.443	27.0487	49.704	20.4094	88.028	30.488	45.000	52.784
9/21/2022 8:36	59843.3587	jw02586403001_03102_00001_nrca3	CCJFOFTLM2022264105229302	g: 72/750	0.033	0.035	1.5	1.02	50.5632	19.4561	50.6266	39.4769	19.5239	41.4832	88.028	30.488	45.000	52.480
9/23/2022 11:23	59845.47471	jw02726137001_03102_00001_nrca3	CCJFOFTLM2022266200529429	g: 72/750	0.03	0.034	1.4	0.81	3.24191	17.6957	17.6111	4.72997	17.7638	17.6478	88.028	30.488	45.000	52.973
9/26/2022 5:51	59848.24437	jw02586368001_03102_00001_nrca3	CCJFOFTLM2022269113518483	g: 72/750	0.031	0.033	1.42	0.87	37.5929	32.4264	37.6569	33.8479	32.4993	33.0179	88.028	30.488	45.000	52.724